T.C.

ALTINBAS UNIVERSITY
Institute of Graduate Studies
Electrical and Computer Engineering

RETINAL FUNDUS IMAGES OF OPTICAL DISK DETECTION

Lina ELWIYA

Master Thesis

Supervisor
Asst Prof. Dr. Sefer Kurnaz

Istanbul, 2021

RETINAL FUNDUS IMAGES OF OPTICAL DISK DETECTION

by

Lina ELWIYA

Electrical and Computer Engineering

Submitted to the Institute of Graduate Studies

in partial fulfillment of the requirements for the degree of

Master of Science

ALTINBAS UNIVERSITY

2021

The thesis titled “RETINAL FUNDUS IMAGES OF OPTICAL DISK DETECTION” prepared and presented by “Lina ELWIYA” was accepted as a Master of Science Thesis in Electrical and Computer Engineering.

Asst. Prof. Dr. Sefer Kurnaz

Supervisor

Thesis Defens Jury Members:

Prof. Dr. Osman Nuri Ucan	Institute of Graduate Studies, Altinbas University	_____
Prof. Dr. Mesut RAZBONYALI	Engineering and Natural Sciences, Maltepe University	_____
Asst. Prof. Dr. Sefer Kurnaz	Institute of Graduate Studies Altinbas University,	_____

I certify that this thesis satisfies all the requirements as a thesis for the degree of Master of Science.

Approval Date of Institute of Graduate Studies:
08/01/2021

I hereby declare that all information in this document has been obtained and presented in accordance with academic rules and ethical conduct. I also declare that, as required by these rules and conduct, I have fully cited and referenced all material and results that are not original to this work.

Lina ELWIYA

DEDICATION

First and foremost, I would like to thank Allah Almighty for giving me the knowledge, ability and opportunity to undertake this research study and to persevere and complete it satisfactorily . Heartfelt thanks goes to my father and my mother. Every success is a direct consequence of their influence in my life and their love. At the end I have to mention my brother and sister for their support and love .

ACKNOWLEDGEMENTS

All praises is to ALLAH Subhanahu wa ta'ala for bestowing me with health, opportunity, patience, and knowledge to complete this research. May the peace and blessings of ALLAH Subhanahu wa Ta'aala be upon Prophet Muhammad (Sallallahu alayhi wa sallam).

My profound gratitude goes to my supervisor Asst. Prof. Dr. **SEFER KURNAZ**, for his invaluable guidance, excellent supervision, continuous encouragement and constant support in making this research possible. His cooperation, tolerance, constructive criticism and useful suggestions have been of immense encouragement to me and enabled me to develop a deeper understanding of this research. I also thank Dr. Alaa Hamid Mohammed I sincerely thank him for the time spent in proofreading and correcting my mistakes.

Finally, I extend my gratitude to all those who were directly or indirectly involved by either encouraging, praying and offering constructive advice in this thesis.

Thank you.

ABSTRACT

RETINAL FUNDUS IMAGES OF OPTICAL DISK DETECTION

ELWIYA, Lina

M. Sc., Electrical and Computer Engineering, Altinbas University

Supervisor: Asst. Prof. Dr. Sefer KURNAZ

Date : 8/01/2021

Pages: 69

The automated segmentation and examination of the retinal pictures requires optical disc(OD) identification. A new technique for border detection of OD from retinal images of the color fundus is proposed in this paper. In combination with the difference Gaussian (DOG) filter, morphological operators and contrast enhancements techniques are used to achieve the OD limits. With a comparable time, we achieve a high success rate with our proposed algorithm. Six datasets available to the public in 1660 images; STARE, DRIVE, ARIA, DIARETDB1, DIARETDB0 and MESSIDOR sets of data. have been evaluated for the performance of our proposed method. Experimental evidence shows a 100% DRI VERY, ARIA, DIARETDB1 and DIARETDB0 image success rate; better than the most advanced methods for ARIA, DIARETDB1, and DIARETDB0 datasets with accuracy below 99%. With the average processing time of 1,2 seconds, the algorithm achieves 98.8% and 99.83% respectively in the STARE and MESSIDOR datasets.

KEYWORDS: Optic disc detection, Optic disc segmentation, Retinal images analysis, Difference of Gaussian filter.

TABLE OF CONTENTS

Pages

LIST OF FIGURES

Pages

LIST OF ABBREVIATIONS

CDR	Cup-to-Disc Ratio
DR	Diabetic Retinopathy
DRIVE	Digital Retinal Images for Vessel Extraction
MESSIDOR	Methods to Evaluate Segmentation and Indexing
OD	Optic Disc
STARE	Structured Analysis of the Retina

1. INTRODUCTION

1.1 INTRODUCTION

Research to discover new techniques to diagnose diseases has been going on worldwide to improve the life of the people as new diseases emerge day after day. The aim of any such research is to diagnose the disease accurately, quickly and economically. The identification of optic disks (OD) is a part of the diabetic retinopathy (DR) screening system. DR is a very common eye condition in the workforce Indians, Europeans and the United States who suffer from type 1 and 2 diabetes and the major cause of blindness, as studied by Maninis et al. (2016) [1]. Effective drugs to prevent the development of the disease are available. Early detection of DR is very necessary therefore, as reported by Tagore et al. (2016) to prolong the development of the disease and postpone blindness [2]. DR patients normally have no visual imperfection until the disease reaches a wide area of the retina. Mass-screening diabetes patients are also desperately needed. A retinal photograph is taken and analyzed, as illustrated by Alam et al. (2016) in order to decide whether a person suffers from DR. A large number of images are needed for the mass screening of patients with diabetes. Manual examination costs preclude the large-scale execution of screening. An automated screening system for retinal images could be developed as a potential solution. Such a device should be in a position to differentiate between DR-impacted retinas from normal Letishia et al. (2016) retinas. Then, only those images detected by the device must be viewed as probably abnormal. As shown by Sedai et al. (2016), this would greatly reduce workloads for ophthalmologists. A variety of different eye diseases can occur in a picture which must be examined by the automated screening system. The automated DR screening method for the retinal image would concentrate primarily on the anatomical structures of the eye, much as Sengar et al. (2016) suggests an ophthalmologist. [3]. However, the retina does not usually catch anatomical objects such as the vasculature, the optical disk and the macula, which are in retinal photography If these structures have been mounted on the image of the device, These positions could be used to detect DR symptoms as landmarks. However, it is not trivial to construct a robust automated OD detection process, as the optical disks will differ in appearance because of the retinal disease investigated by Sharma et al [4].

1.2 BACKGROUND

Independent scientific and engineering areas are increasingly expanding the application of image processing and vision techniques in machine. In the medical sector, new advances in such approaches specifically seek to identify medical conditions early by reducing the time for disease detection in order to prevent the disease from emerging. The image processing, such as the automated diagnostics systems, has been successfully developed. These systems are based on an invasive diagnosis of diseases in a short period of time These systems are. In order to detect diabetic retinal funduage images, for instance, a number of automated systems have been suggested. This is a short description of the retina, fundus imaging and diabetic retinopathy.

1.2.1 Anatomy of Human Eye

The eye is a main organ that makes it possible for humans to look, respond and adjust to their surroundings. It also allows for the representation of visualized object types, colors and dimensions. Three main layers of the eye are presented: cornea sclera in the outer layer, choroid vascular layer and retina neurosensory. Even a color (blue, green, brown or blend), iridescence and the normally black opening are the most visible aspects of the eye. An image-focusing light ray passes through the cornea (Goran et al. 2011) pigment epithet [5]. Figure 1.1 shows the anatomy of the human eye.

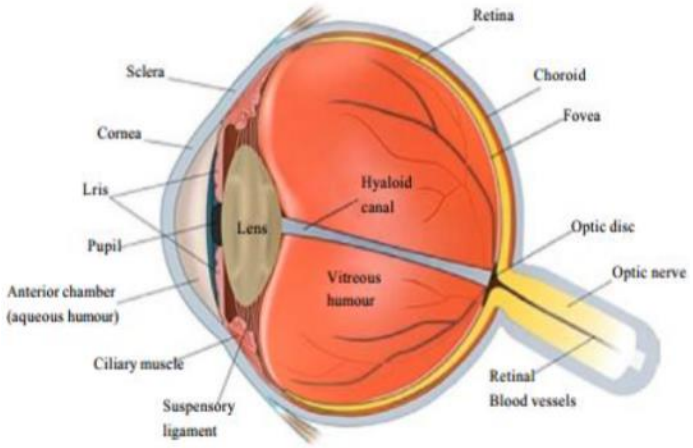

Figure 1.1: Anatomy of human eye [5]

1.2.2 The Effect of DR on the Retina

Diabetic retinopathy (DR), if not initially analyzed and diagnosed as studied by Parthasarathi et al. (2016), is an extreme retinal disorder, related to mellitus diabetes, this is the key cause in most countries of partial or even complete vision loss. Diabetic retinopathy does not show any symptoms in pathogenesis before the end. Testing diabetic patients for the presence of diabetic retinopathy and development of diabetic symptoms will reduce by 50% the risk of blindness. The patient ratio of ophthalmologists is smaller, and thus the treatment of all patients, as shown by Sharpe et al. (2016) is unsatisfactory. Sometimes the retinopathy screening requires skilled labor and manual procedures that can lead to cost and time, as Zhang et al. (2016) explained [13]. The need for automated early detection methods is important as the numbers of people affected by diabetes worldwide increase. Automated early detection can also monitor the acute condition and help eye doctors investigate and manage the disease more effectively, as illustrated by Singh et al. (2016) [14]. In order to automatically locate a device, the digital images of the retina defined by Sudeshna et al. 2016 can be found and manipulated)) [15]. Two main phases of diabetic retinopathy (NPDR) and diabetic proliferative retinopathy (PDR) are usually known as diabetic retinopathy. NPDR has also, as summed up by Wilkinson et al. (2003), been graded into mild, moderate or extreme levels. Figure 1.3 illustrates the DR phases in retinal pictures.

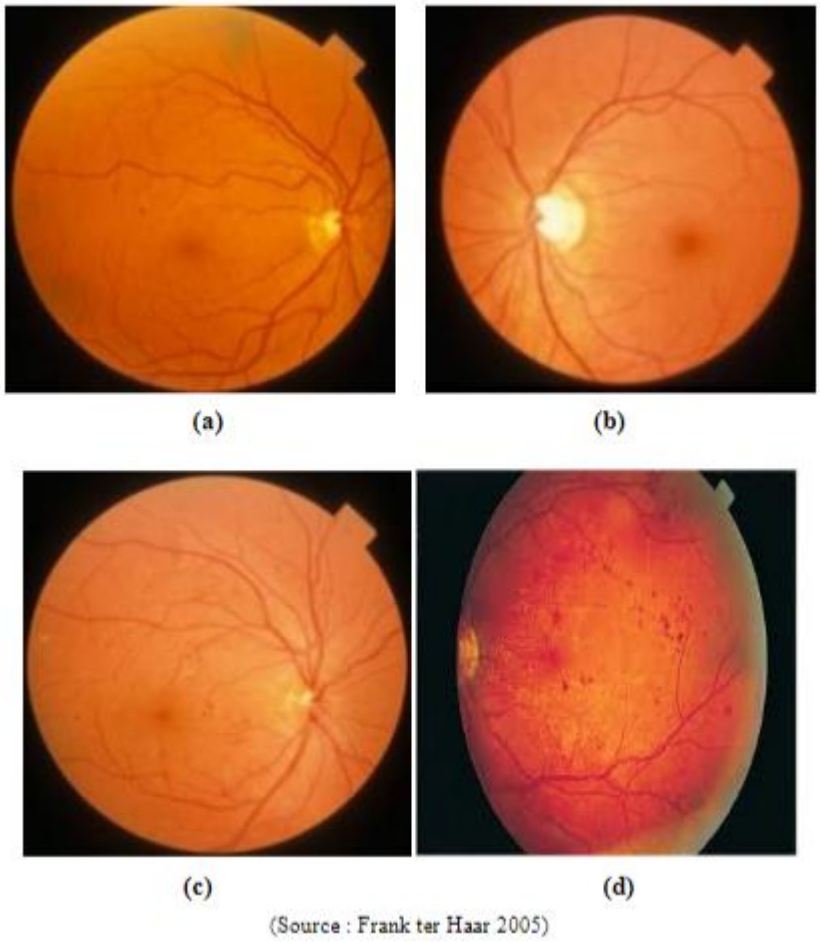

Figure 1.2: Stages of Diabetic Retinopathy (DR) (a)Healthy image (b) Mild DR (c) Moderate DR (d) Severe DR

The severity scale developed for DR and diabetic Macula Edema (DME) was shown in table 1.1 according to the international clinical disease scale.

The appearance of the human retina is impaired by symptoms of DR. In the first stage a retinal photograph reveals just a few signs of DR (see Figure 1.5). Additional signs become evident as the disease progresses.

- Early No proliferative retinopathy: at this earliest stage micro-aneurysms occur. They are small regions where the blood vessels of the retina are globular and small.

- Advanced Retinopathy Non-proliferative. Some of the blood vessels supplying the retina are blocked as the disease progresses.

Figure 1.3: Disease severity scale

Retinopathy Stage	Findings on Ophthalmoscopy
No apparent retinopathy	No abnormalities
Mild non-proliferative DR (NPDR)	Microaneurysms only
Moderate NPDR	More than just microaneurysms but less than severe NPDR
Severe NPDR	Any of the following: 1. More than 20 intraretinal haemorrhages in each of 4 quadrants 2. Definite venous bleeding in 2 or more quadrants 3. Prominent intraretinal microvascular abnormalities in 1 or more quadrants and no signs of proliferative retinopathy
Proliferative DR (PDR)	One of the following: 1. Neovascularisation 2. Vitreous/preretinal haemorrhage
Advanced Diabetic Eye Disease (ADED)	One of the following: 1. Formation of fibrovascular tissue proliferation 2. Traction retinal detachment due to formation of posterior vitreous detachment 3. Dragging of retinal/distortion 4. Rhegmatogenous retinal detachment

- Extremely advanced non-proliferative retinopathy. More blood vessels and blood are obstructed supplies are robbed in some sections of the retina. The areas are called cotton-wooden patches. These areas are white and yellowish. The cotton wool spots give the body signs for fresh blood vessels to be fed.

-Retinopathy of proliferation. The signals sent by the retina for nutrition in this advanced phase activate the growth of new blood vessels. Proliferative retinopathy is called this condition. The new vessels of blood are irregular and weak. The retina and the glass gel surface lining the eye. are rising. Such vessels do not cause signs or loss of sight in their own right. They have small, delicate walls, however. A significant loss of vision and blindness can occur when they leak blood.

The progress of DR phases which could lead to blindness is shown in Figure 1.5. Step I: Early Retinopathy No proliferative. Step II-III: Progressive Retinopathy Non-proliferative. Step IV: Retinopathy of proliferation. Blindness may occur after stage IV.

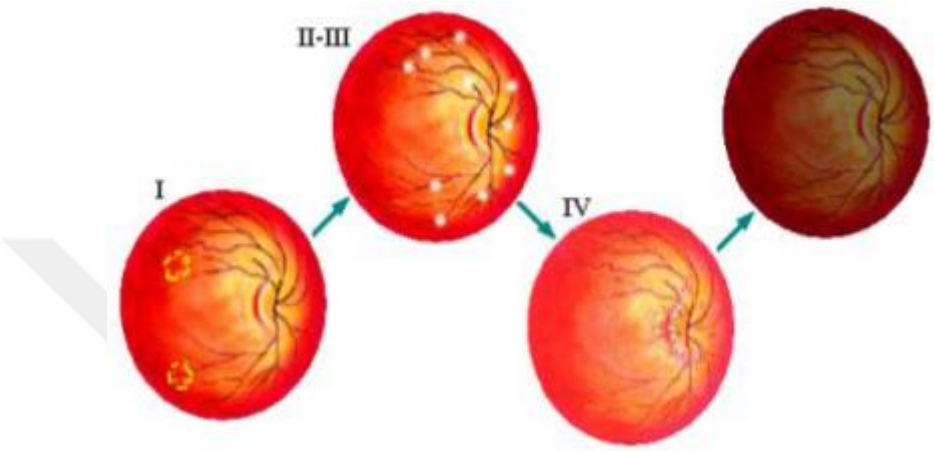

Figure 1.4: The progress of DR stages

1.2.3 The Retina

The retina is made up of neurons, cell supporters and photoreceptors. It is a metabolized organ, which is highly susceptible to nutrient which gaseous exchange and diffusion. As light rays penetrate the eye that concentrates on the retina, the retina responds, sending it through the optic nerve to the brain. The brain then recognizes them as an image.

The retina has two sources of blood: choriocapillaris and central retinal artery branches. A third of the retina is provided by the choriocapillaris, while two thirds are provided by the branches of the central retinal artery [1]

1.2.4 Fundus Photography

Various medical imaging techniques, including fundus photography and OCT, are used to image human eye internal structures. These two methods are non-invasive. The OCT offers transversal eye tissue images. Nevertheless, fundus images contain pictures from Human eye internal structures such as the retina, optic disks, macula, fovea and vessels of the blood [2]. The OCT facilitates tissue eye disorder diagnosis. Fundus images are, however, very useful in diagnosing

retinal eye disorders. In addition, fundus photography is the fastest and simplest process. It is used to diagnose eye disorders, observe a wider area of retina.

Fundus pictures are all indexed or RGB pictures of varying intensities (Red, Green and Blue) [2]. These images are present in various public retinal photo databased applications, including DIARETDB, the Digital Retinal Image for Vessel Extraction (DRIVE), and the Regular Diabetic Retinopathy Database (DIARETDB). These databases contain standard as well as irregular retinal images. Although STARE data database contains 400 images of different eye conditions, the high signal to noise (SNR) for most DR-related images. DRIVE pictures, the fact that they are limited to 40 frames, instead, is not taken into account. Consequently, in this study DIARETDB is the main archive, as it contains more than 200 low-signal noise images.

1.2.5 Retinal Imaging

Visualization and computer vision methods are becoming more and more popular in all medical sciences when processing images. They are important in modern ophthalmology because they rely on visually-oriented signs. In the last ten years, retinal image studies have been commonly used to diagnose and track the development of many diseases in the medical community. The scope for these technologies in ophthalmology has increased as digital imaging and computing power expand more and more.

The development of automated diagnostic systems such as diabetics, macular degree correlated with age and premature retinopathies in ophthalmic imaging over the last 15 years has included. These diagnostic systems provide the opportunity to use broad-based screening services which save substantial money and Kittipol et al. (2014) is free from observer exhaustion and exhaustion. [16].

Retinal imaging for retinal patients and systemic disorders is the basis for clinical treatment and management. There is a great interest in the ability to picture the retina and to improve image analyzing techniques. Since the retina needs to see the outside world, the eye structures involved must be optical transparent to form an image. Thus, the retinal tissue and the brain tissue, which is noninvasively demonstrated by Ganesh babu etc. (2014) can be visualized from the outside with suitable techniques. [17].

The use of digital retinal image analysis is increasingly common and offers sophisticated techniques to analyze various aspects of vascular retinal topography, such as the length and widths of retinal micro vessels. Ophthalmologists conventionally imaged the eye using ophthalmoscopes in determining the health conditions of the retina. But abnormalities are often restrained and may be missed by visual observation or conventional retinal image inspection.

The most consolidated way of retinal imaging is fundus imaging. Until recently, the only source of quantitative indications representing retinal morphology was fundus image analysis. Fundus photography techniques include (including so-called red-free photography), Color fundus imaging, imaging stereo fundus, hyperspectral imagery, ophthalmoscopic (SLO) laser scanning, adaptive optics (LOS), angiography with fluorescence and angiography of indocyanines as stated by Hafsah Ahmed and others.

In fundus photography, the retinal images are acquired with a medical device known as a fundus camera made of a powerful digital camera with a special optics. The 3-D retinal semitransparent tissues projected in the imagery plane are replicated with a 2-D representation using the reflected light of a particular waveband. The size of the picture in this 2-D picture is the reflected light.

Color fundus photography displays the intensity of the images as determined by the sensor's spectrum sensitivity. In red, Green and Blue wavebands Imaging intensities represent the sum of reflected light from two or more different angles of view to depth resolution in stereo fundus photography. Image intensities display several wavelength bands with the reflected light in hyperspectral imaging.

In SLO, the image amplitude is the sum of reflected laser light from a single wavelength in a time series. In adaptive SLO optics, the image intensities indicate the sum of the laser light reflected in the wavefront modeling. The picture intensities in fluorescein angiography and indocyanine angiography reflect the quantities of fluorescein or indocyanine green fluorophobic photographs emitted by Abramoff etc (2010) to subjects in circulation.

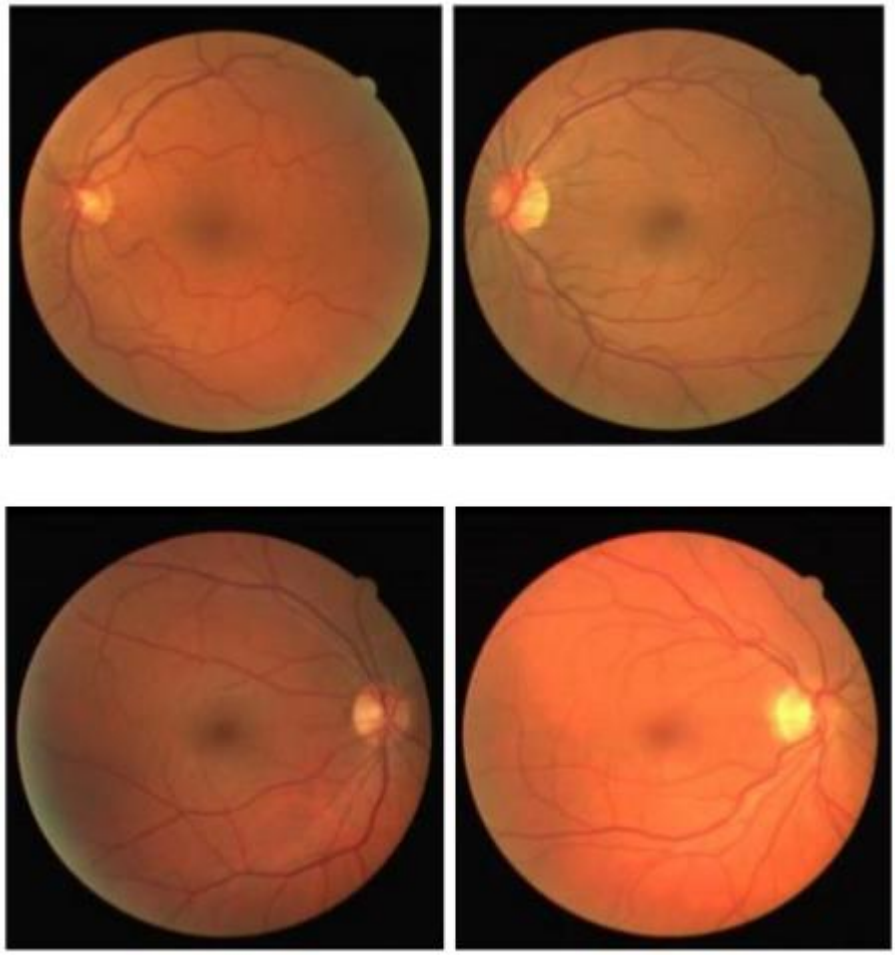

Figure 1.5: Representative normal retinal fundus images (Source: DRIVE database, Neimeijer et al. 2004

Figures 1,2 and 1.3 respectively show representative normal and abnormal retinal fundus images. Because the retina is not usually illuminated internally, external light and reflected light must pass through the pupil's plane. The scale of the pupil was therefore the key technological challenge of the fundus imaging, usually about 2 and 8 mm in diameter. The fact that the illumination and imagery beams cannot match is complicating fundus imagery.

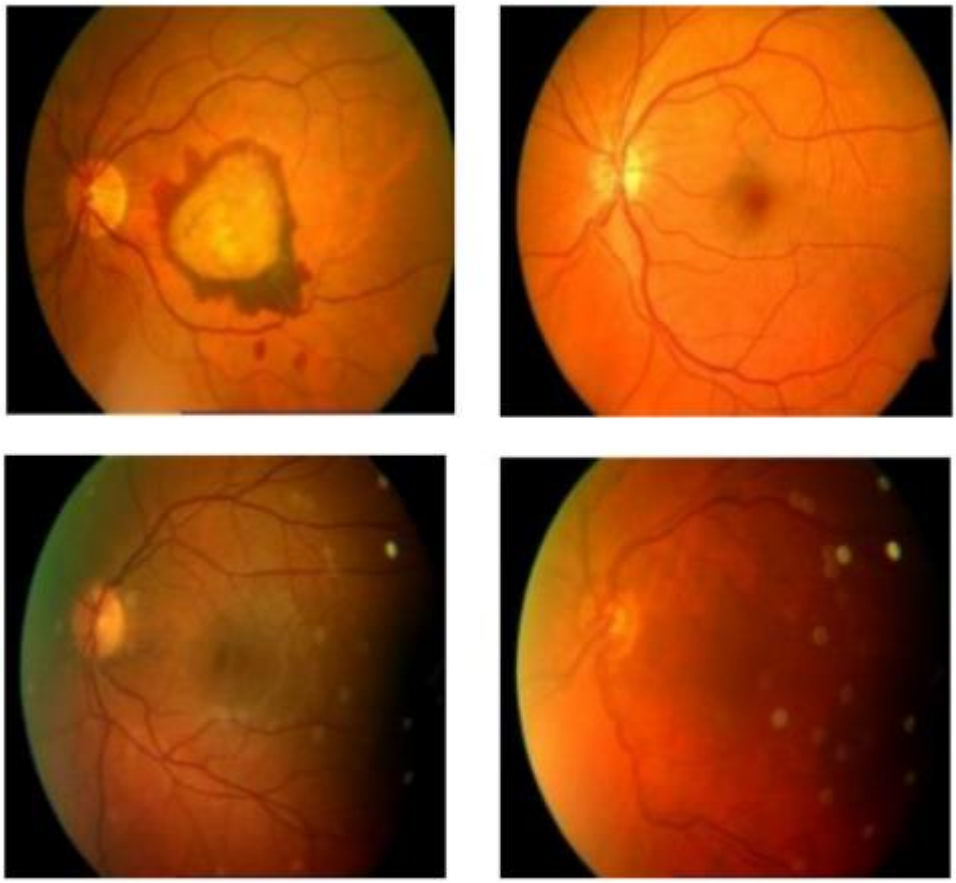

Figure 1.6: Representative abnormal retinal fundus images

1.2.6 Diabetic Retinopathy

The effect of diabetes on the eye is diabetic retinopathy (DR). Blindness is caused by number one eye disorder. It is more likely that patients with diabetes become older than those with diabetes. Early DR signs are microaneurysms, bleeding and exudates.

DR starts when diabetes mellitus causes slight swelling of the minute blood vessels on the side to induce microaneurysm retinal blood vessels (MA). With the damage on the eye, it causes deep hemorrhages. Retinal hemorrhage can lead to serious problems with vision. As this disease progresses, the retina responds by forming blood vessels that are abnormally thin, Leaky, delicate and erroneous. The more abnormal veins, the more the retina they bleed. The more they expand.

In addition, the sediments consisting of lipid byproducts called exudates are formed by the leaked liquid. Yellow exudates occur in different sizes and locations in the retina. [3]

The No proliferative (NPDR) and Proliferative (PDR) forms have two major forms. The condition is proliferative and neovascular when an irregular blood vessel develops in the eye. In case of non-proliferative growth of the irregular blood vessel, the disease falls into mild, moderate and extreme categories [1]. The picture of a retinal fundus with DR is shown in Figure 1.8.

Since patients may not have vision problems before treatment is failing in late stages of illness, diabetic retinopathy is unparalleled. Therefore, it is important to diagnose DR early and it is beneficial to prevent the disease from progressing. Furthermore, an annual eye examination for diabetic patients is very relevant [1].

With the aid of manual blood segmentation and lesion extraction, the human eye can detect DR from retinal fundus imagery. However, this process is a very long one involving preparation and could be influenced by the fatigue of the observer. Researchers have therefore proposed numerous solutions for the automatic detection of DR.

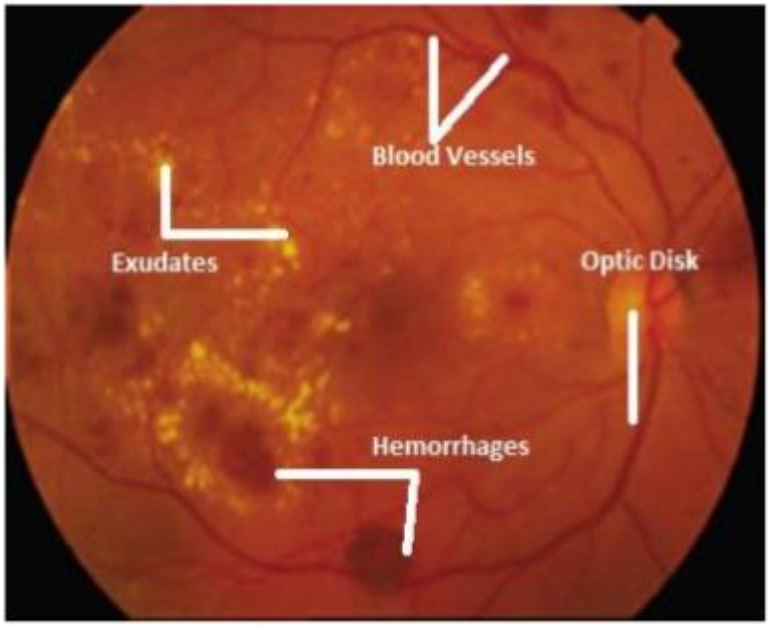

Figure 1.7: DR Lesions Retinal Fundus Image.

Figure 1.8: The Author's fundus picture was taken in the Toronto health one clinic during the February 2016 vision test.

1.3 EXAMINING THE HUMAN RETINA

The macula is the human part of the retina that was found during the day. DR damage can cause significant loss of vision. Fresh blood vessels are to expand in the OD area in the event of proliferative-DR. The retinal region of the macula and the optical disk region are the priority for the ophthalmologist when a retina has to be checked. Four or more photographs of the retina of the patient must be taken during an eye test; Anatomical structures such as the macula, the optic disk and blood vessels may contain a healthy retinal image. A noticeable signs of eye-disease may also be present in a picture of the retina. Typically, the optic disk and/or macula is in the retinal picture. In relation to the optic disc, the eye-type (left / right) defines the orientation of the macula. The macula is on the right of the optical disc in the retinal image of the left eye, while the Macula is on the left of the optic disk in a photo of the right eye (figures 1.10 and 1.11 show). The optic disk appears as a glossy yellowish circular object in a healthy retinal frame, which is partly hidden by vessels. However, due to the photograph, the entire retina and the optical disk can vary, just like a normal photograph. For example, a photograph may be illuminated unevenly, resulting in

an OD appearance less distinct, or it may be broken, as shown in Figure 1.12. Diseases can impact the appearance of OD as well: proliferative DR results in a vessel-covered optic disc. Figure 1.13 provides several examples of images in the optical disk that are different from normal. The optical disk is different in appearance of the image, size and position when creating an automated OD detection procedure.

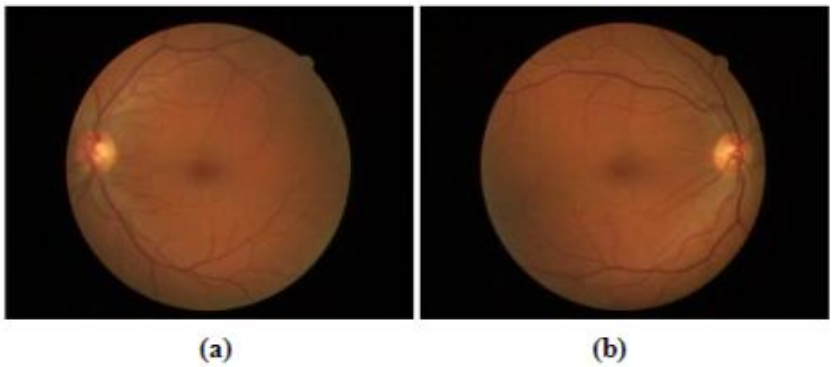

Figure 1.9: A healthy macula centered retina (a) left eye (b) right eye (Source: Frank ter Haar 2005

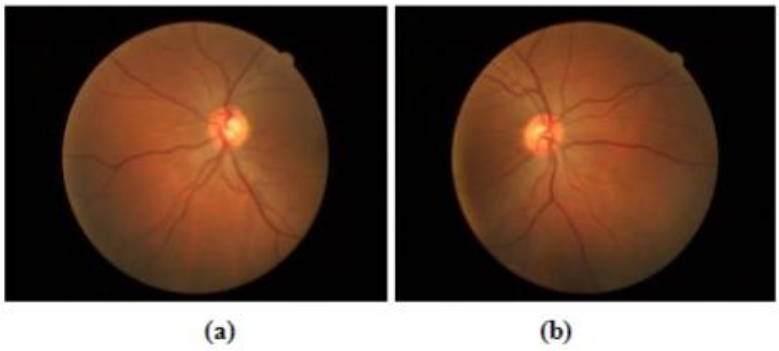

Figure 1.10: A healthy OD-centered retina (a) left eye (b) right eye (Source: Frank ter Haar 2005)

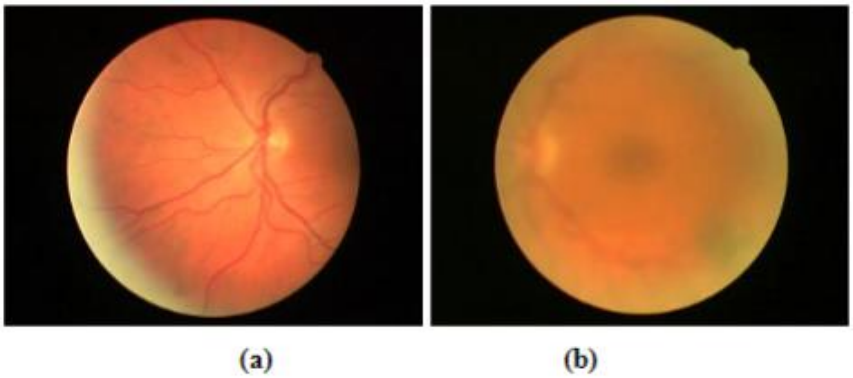

Figure 1.11: (a) An uniformly illuminated image. (b) A dull picture (Source: Frank ter Haar 2005)

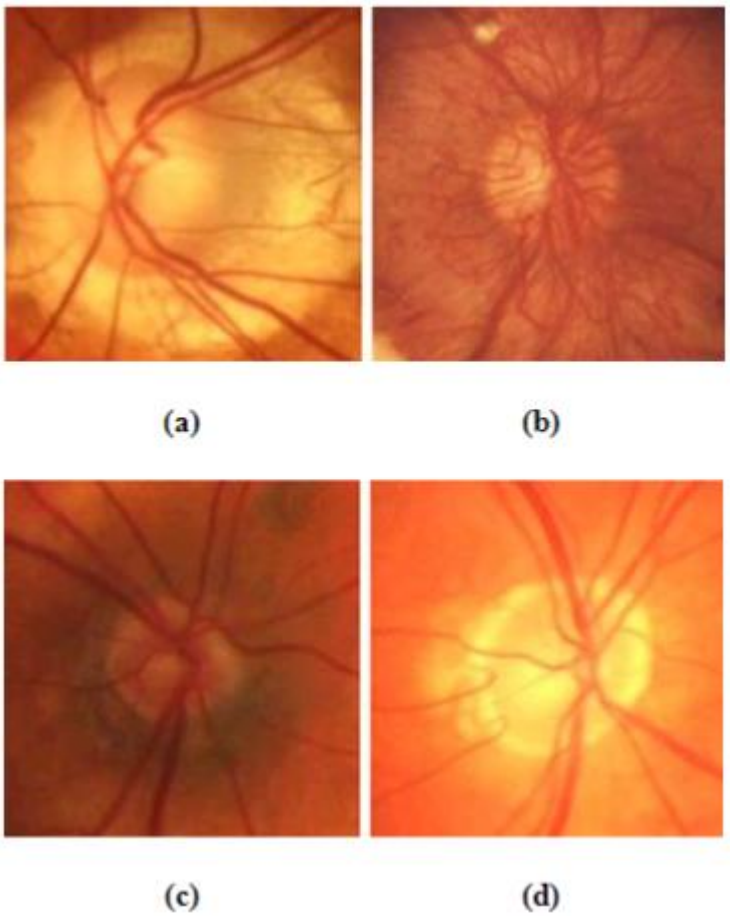

Figure 1.12: Diverse appearance of the optic disc

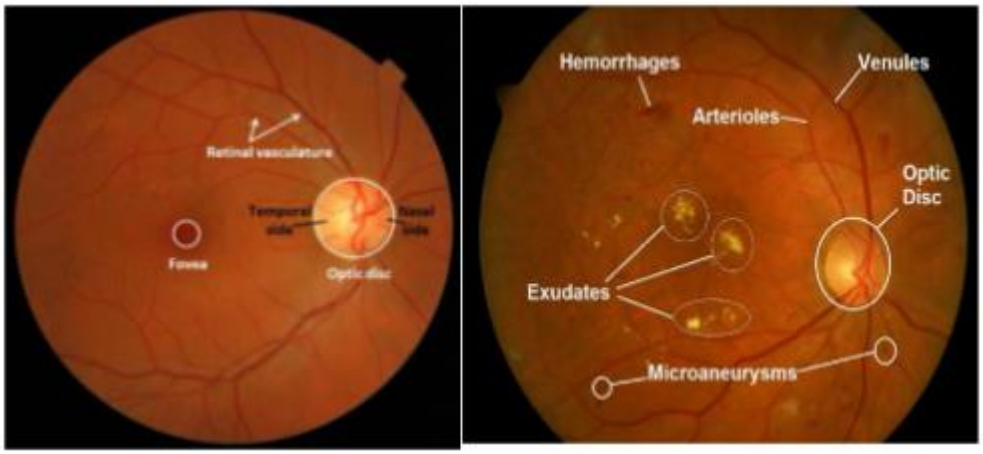

Figure 1.13: Retinal image Landmark (Source : Abdullah et al. 2016)

The OD is the lightest part of the ordinary fundus and has a somewhat oval (elliptical) vertical form. The OD is shown in bright yellowish or white pictures, as shown by Figure 1.10.

OD is a blood vessel exit area and is also characterized by relatively pale vision in the vision of the retinal neuron tissue. Relatively measured in the retinal fundus picture, Jun cheng et al. (2014) The entire framework occupies approximately a seventh [18]. Li and al. The OD sizes of the picture vary from person to person and cover between one-tenth to one-fifth.

The OD detection / location mechanism only detects the centroid (center) of the OD. The OD is positioned automatically. The purpose, however, of discord detection is to divide the OD correctly the edge between the retina and the nerve heads is detected (neuroretinal rim or optical cup).

1.4 RESEARCH PROBLEM

The picture of retinal fundus is commonly used in the diagnosis and treatment of eyelid diseases including diabetic retinopathy and glaucoma described by Li Xiong et al. (2016) [20]. Retinal image processing has significant implications for eye care and for the clinical trials specified by Kemal et al. (2016) [21]. Retinal image processing has great consequences in the field of eye treatment. Normally retinal images are manually graded by clinicians in a time-consuming process. Prior to specialist inspection of an eye, a computer-aided analysis could provide an immediate detection and characterization of retina features represented by Karkuzali et al. (2015). Segmenting the optical disc's geometric form and the scale and anterior segmenting of the irregular growth of any area in the eye play a major role in measuring. The exact location, position and area values for a contour and structural part of an image needed by ophthalmologists created by Behdadet al. (2015) are determined automatically. But several difficulties such as initialization, optimisation and inadequate results in bright image are posed in these segmentation methods. Segmentation is therefore a problem for the researchers in retinal imaging.

1.5 IMPORTANCE OF OPTIC DISC DETECTION AND SEGMENTATION

The Optic Disk (OD) is regarded by retinal fundus image as a major function. OD Identification is the main component of preprocessing in many of Kemal et al.'s (2016), A module shared with most retinopathy systems for anatomical structures and lesions automated extraction. The OD also

marks the other properties of fundus, including the relatively stable space between the OD and the main macula (fovea) for estimating the position of the behad et al. (2015) macula. The OD was also used to map retinal vasculature as an initial point for Avinash et al. (2014) [22] tracking techniques. Large vessels in the OD region can be used to monitor the vessels as a seed.

Automated segmentation of the OD-rim / cup / boundaries is important for detecting OD-related abnormalities. E.g., Kemal et al. (2016) specified diabetical retinopathy, glaucoma, disco neovascularization (NVD) and papilledema. Different pathologies, especially for glaucoma, were seen in Joshi et al. (2011) [23] to indicate changes in form, color, or depth of OD. The measurements of ODs are also used to calculate anomalous characteristics attributable to such retinopathies, such as glaucoma and Avinash etal. diabetic retinopathy (2014). Moreover, the OD may initially be recognized by Jun-cheng et al. as "one or more" candidate, since the color of the OD was close to that of the Yellow exudates, and region One lesions occurring in diabetic retinopathies [25] could be recognized. Identification and elimination of the OD enhances the classification of the Ana et al. exudate regions (2014) [25].

1.6 OBJECTIVE OF THE RESEARCH

The main purpose of the research is to locate Optical Disk in the images of the retinal fundus. The particular research aims are:

- To detect and segment optic disc in the retinal fundus images using directional matched filtering and operator splitting approach respectively
- To use freely accessible and in real time retinal image data sets to validate the proposed method.
- Compared with other state of the art techniques.

1.7 CONTRIBUTION

This study proposes a new algorithm to detect the OD border, obtained via morphology and contrast increases, using two OD-related sigma values, threshing areas and selecting circular object zones, then apply the Gaussian Differance (DOG) filter. This analysis is also available in the

following report. The first to be checked with the 6 publicly accessible databases is the algorithm proposed. Experimental findings indicate good performance with a reasonable processing time compared to literature methods.

1.8 ORGANIZATION OF THE THESIS

This study is organized into 4 chapters: the introduction, objectives and significance of OD detection and segmentation is discussed in Chapter one. The literature review and the fundamental principles for automated localization and segmentation of OD are discussed in Chapter 2. The materials, the suggested approach and a description of the material used are described and the findings presented and Chapter 3 includes discussions and comparisons. Lastly, Chapter 4 provides the conclusion and potential work of the study

2. LITERATURE REVIEW

2.1 BACKGROUND

In literature the location of the optical disk is typically identified as the identification of the disk center either by indicating the center of the optical disk or by inserting a mask into a certain area in the retina. The optical disc segmentation generally refers to the subsequent role of the contour determination. The retinal image analysis has essential tasks to locate and segment the optical disk. The middle and the contour of the disc are also important points for setting a benchmark for retinal anatomy and pathology.

The first step is to assess the defects of the retinal system, such as drusen, exudates, microaneurysms and bleeding, as well as imaging objects such as hazelnuts, candles, woolen locations, and uneven human eye lighting. Optic disk detection This chapter addresses some recent methods for detecting and segmenting optical discs in the literature.

2.2 OPTIC DISC DETECTION

Kemal Akyol et al. in retinal images of noise and other lesions (2016) proposed optical disk position approach Five major steps are being proposed the process: image processing, extraction of key points, texture analysis, visual dictionary and techniques for classification.

Li Xiong (2016) proposed locating OD with pathologic changes in the retinal picture. The method consists mainly of three stages: Regional Interest Identification (ROI), candidate pixel identification and confidence score calculation. In the proposed approach to OD location, the properties of direction, intensity, OD and size of the vessel were extracted and used.

The multi-determined OD band filter has been proposed by Behdad et al. (2015). Circular Hough transform for OD detection was used by Caroline et al. (2015). By adaptive morphological approach, Gonzalez et al. (2014) located OD The Hough Transform used by Arriaga et al. [26] was accompanied by an active segmentation contour model. Avinash et al. (2013) suggested a nearest Neighbour OD detection algorithm. Intelligent fusion of optical disco localization methods in retinal funded images was proposed by Zhang et al. (2013) [27].

Angel Suero et al. (2013) [28] suggested a technique consisting in the strength of dimensioned images and an optical disk position in high-resolution images to homogenize the context and collection of morphological opening and closing operations.

Deepli et al. (2012) proposed an ensemble based automated approach to detect OD and its center for both normal and abnormal retinal images. Dehghani et al. (2012a) [29] proposed two methods to localize center of OD. The first one is based on corners and bifurcations obtained using Harris corner detector, the second one (Dehghani et al, 2012b) is based on histogram of each color component as template. Yu et al. (2012) [30] proposed a OD location in which images are identified using template matching and model parameter estimation. The template has to be modified to various picture resolutions. Vessel features (patterns) on the OD are then used to evaluate the position of OD. Jaspreet kaur et al. (2012) [31] developed a method to detect location of OD by optimum threshold algorithm.

The method of finding OD for Asians through multiscale Gaussian filtering was developed by Bob Zhang et al. (2012) [32]. This process supplements current algorithms by using two steps, such as the identification of OD vessels and the matching of OD vessel candidates. The first step is rendered with Gaussian multi-scale filtering, scale production and double thresholding to first draw a directional map of the vessel of different thicknesses. The map is then diluted until another threshold is used to delete low-intensity pixels. The OD vessel candidates are then created. In the second point, the candidates are given different dimensions and the pixel with the smallest difference is the OD middle. Another approach based on peripapillary elimination atrophy is proposed by Jun Cheng et al. (2012). The removal takes place through edge filtering, elliptical transformation of Hough restriction and peripapillary atrophy detection. With the exclusion, edges that are potentially from non-disk structures, in particular peripapillary atrophy, shall be removed to improve the segmentation accuracy. The automated device of Goatman et al. (2011) [33] is able to differentiate normal vasculature from abnormal optic disks. This may be part of a manual grading system or an instrument for prioritizing queues for patients.

Lu & Lim (2011) [34] is a line operator designed to reliably locate the OD from retinal images. In the position of linear image structures from various forms, line operators were used. Joshi et al. (2010a) proposed a technique based on segmented OD and cup areas obtained from monocular retinal images that incorporates local image information in multi-dimensional feature areas around each point of interest, to provide a solid response to changes found in the OD and around the region. The technique of the OD detection using image analysis of contrast and structures was proposed by Arturo et al. (2010).

The model-base methodology to protect OD from digital retinal images was introduced by Arturo et al. (2010) [36]. The Circular Hough transformation employs morphological and edge detection techniques for approximating circulatory OD limits. As an initial information, a pixel within the OD is required. A localization technique is also suggested for this purpose based on a voting-type algorithm. Ahmed E. Ahmed E. Mahfouz et al. were presented with a technique based on two projections of certain picture function encoding x and x- OD co-ordinates. (2010). (2010). To decide the location, 1-D screenings are searched. This eliminates 2D image space and enhances the phase of OD positioning.

Rather, Tobin et al. (2006) [38] suggested a system focused primarily on vasculature-related OD characteristics. In red-free images each pixel was labeled in OD or non-OD by means of a probability distributed that defines the luminance within the retinal retina and density, average thickness and average orientation of vasculature.

OD was detected using a method of detecting geometric forms in an image. Hough transform; Morris et al. are used for the Circular Hough transformation (CHT). [39] Approximately circular OD detection. The retinal vasculature was separated from the Greenband picture with the morphological closing operator. On the edges of the image the Sobel operator and the simple threshold were used. The CHT was used on the margins and the biggest cycle matching the OD was created.

Based on the above review the researchers Kemal Akyol et al. (2016), Jielin Zhang et al. (2013), Yu et al. (2012), Lu & Lim (2011), Joshi et al. (2010a), Mahfouz et al. (2010) considered the OD as the brightest region within retinal image. The researchers Bob Zhang et al. (2012), Jun Cheng et al. (2012), Arturo Aquino et al. (2010) considered the OD for dark and diseased images like diabetic retinopathy. Researchers Li Xiong (2016), Behdad et al . (2015), Caroline M et al . (2015), Gonzalez et al . (2014), Arriaga et al . (2014), Avinash et al . (2013) interpret the OD as the region of neighboring pixel intensity with the highest difference in intensity. For regular, healthy retinal images, both conditions are considered. Deepli et al. (2012). However, OD detection algorithms also failed to demonstrate dark and disordered retinal images. (2011), Joshi et al. (2010b), Siddalingaswamy et al. (2010). This is why ODs with less calculation time and high success rate are suggested with directionally matched filters.

2.3 OPTIC DISC SEGMENTATION

Segmentation of the optical cup for assessing the imagery of human eyes, such as smoke, laceration and irregular lighting. Some approaches have been discussed here for OD segmentation.

The Gradient Vector Flow (GVF) segmentation model used by Caroline et al. (2015) [41] is used for optical cup segmentation. Karkuzhali et al. (2015) [42] has an OD segmentation algorithm fully automated for screening retinal disease. The first step is to eliminate noise by correction of illumination and improvement of contrast. Secondly, an entry-level technique is used using the intuitional fuzzy set of Atanassov (AIFS). The method uses AIFS histone, which contains the pixels in a ruggedness index AIFS histone & histogram with upper and lower approximations. The histogram is the pixel of the pixel range of identical pixels. The optimum value of the threshold is calculated by which pixel the background or object is (OD).

The OD division proposed by Function Match (FM) technique was proposed in Pradhepa et al. (2015) [43]. The matching of the OD and any image input to the OD is detected by FM. This correspondence distributes patches of the input image nearest to patches in the image of reference.

The Automatic Segmentation of Optic cup (ROI) based segmentations method is proposed by the company Ganesh babu et al. (2014) [44]. It can be used to segment the neuro retinal rim automatically. In the Optical Disk area, blood vessels are divided by the threshold of local entropy. The ratio of the upper and lower upper blood vessel region to the lower upper nasal temporal side of the neuro-retinal and the upper neuro retinal rim to the CDR classifying the depth of the context.

Sparse dissimilarity, minimal coding by Cheng et al. (2014), segments and reconstructs the OD. It takes into account the limit of dissimilarity and the limit of sparsity in order to shape a number of reference disks. Cheng et al. (2013) suggested a super pixel classification for glaucoma screening optic cup segmentation. In the segmentation of optical disks, histogram and central surround statistics are used to identify each super pixel as a disk or not. The consistency of the automatic optic disk segmentation is evaluated by a self-assessment reliability ranking. The positioning information is also included in the function space for segmenting the optical cup in addition to histograms and center surround statistics. Early DR identification decreases the possibility of diabetic patients losing their vision.

Zhang et al. (2013) [45] proposes the combination of maximal vessel traversing, multi-channel threshare and vertical and horizontal area of interest to three smart fusion methods. Mudassar et al. (2013) employees in the OD and fovia section use the principal component analysis techniques (PCA). The differential windowing operation used by Kavitha et al. (2013) [46] for the extraction of the optical disc boundary in fundus images in the polar coordinate domain. The exact cup segments based on PCA mathematical morphology were proposed to Sandra Morales et al., (2013).

In order to provide robotic effects of variances found in and around the OD region, Falun Dafa and al. (2012) proposed a model regional active contour using local image details in the multi-dimensional feature space at each point of interest. This model specifies a local energy function for the desired segmentation of ODs. The level set approach reduces this energy to the OD boundary. Additional constraints of knowledge-based clustering and smoothing updates were imposed in order to minimize false discharge, which was also a deformable model suggested by Xu et al . (2012). Their approach achieved a success rate of 94 percent on 100 pictures. When the images had wider and lighter areas than the OD, the segmentation failed. In presence of atrophy, Joshi et al. [47] have tried to segment OD. By using the local red channel intensity and two textured rooms in close proximity of the interested pixels, the regional model has been improved. 138 retinal photographs with 30 Au Field of View (FOV) have been tested in quarantines. Their pattern is based upon the premise that an OD with an atrophy has different textural characteristics than a healthy OD. However, due to the heterogeneity of OD, particularly after the removal of morphological vessels, these differences may be too responsive. This is a costly strategy, since two local features are used.

When pathological regions occur in retina pictures, the OD segmentation methods have failed. Many of these approaches failed due to operator acquisitions and the functional selection errors. (2015, Mudassar et al. (2013), Kavitha et al. (2013), Sandra Morales et al. (2013). Some other approaches have been covered by high computational costs: Jun Cheng et al. (2014), Jielin zhang et al. (2013), Kavitha et al. (2013). The resolution and comparison of some of the Karkuzhali et al. (2015), Xu et al. (2012), Aquino et al. (2010) methods failed. Many cup segmentation procedures took Gradient Vector Flow (GVF) and an active contour model to the edge of the Mary and others picture segment maps. (2015), Ganesh babu et al. (2014), Jun Cheng et al. (2013), Jielin

Zhang et al. (2013), Vasanthi et al. (2012), Joshi et al. (2012). Leakage problem in the weak edges of the images is the principal weakness of the GVF model. The edge map therefore cannot be clearly segmented. Thus, the optics segment disc with better measurements compared to other state-of-the-art approaches, optical disk divisions approach is proposed.

2.4 RELATED WORKS

In the past decade, there have been many methods of image processing for the identification and classification of DR lesions into PDR or NPDR of various forms. These methods are based on many algorithms as DR has two indications. Moreover, the images need to filter out the blood vessels and the optical disk. Following the detection process, most scientists categorized DR using different algorithms.

2.4.1 Hemorrhages segmentation

The segmentation of hemorrhages therefore was the principal goal of a variety of previous research articles. Retinal bleeding was one of the major abnormalities in DR. For example, Kleawsirikul et al. [48] has an automated algorithm for detection of hemorrhages by means of transforming the morphological cap, a filter that binarizes the image by separating the image from closing to opening the image. Blood vessels and leakage were shown by white pixels, and image background was shown by black pixels. Then colour, zone, eccentricity and compactness characteristics were extracted and hemorrhages were categorized according to rules. The accuracy of the hemorrhage classification was 99.12%. However, this work 's sensitivity is weak, just 80.37%. This work also has the benefit that only 20 images are considered.

A different hemorrhage segmentation technique was proposed in [49]. The procedure was based on blood vessels being separated from the image. The blood vessels have been identified using morphological openings with multi-scaling structural elements. The picture was then taken from the blood vessels. There was therefore a segmentation of only hemorrhages. Such an approach has attained 87.69 percent sensitivity. The benefits of MA segmentation are also the early indicator of DR. This study fails, however, to take into account the methodology's consistency test. Precision is an important consideration to assess the efficiency of algorithms.

Future technique was used to segment major hemorrhages by Athira and Ferlin [50]. The technique is based on the division of the image into splat segments. Pixels of the same color and position are found in the splat. Each splat has extracted a wide range of features. In order to pick the best splat function, the mean filter has been used. In fact, this work has the advantage of segmenting large blood vessels. Athira and Ferlin did not include pre-processing methods, calculating sensitivity or measuring accurate data.

The splat technique used by Inbarathi et al. to detect DR [51] has also been used. Furthermore, it was used for section hemorrhages in the Support Vectors Machine (SVM). Contrast, similarity, energy and homogeneity characteristics have been considered. Although sensitivity and precision have not been shown in this research, good results were achieved with respect to the segmentation of hemorrhages. The number of features selected was however limited.

In order for hemorrhages to be identified, Reshma and Chavan [52] developed an automated technique of template matching and regional development. The template correspondence was used to provide information on object centres. In order to segment the correct hemorrhage scale, the rising region technique was used. Classification of NPDR Fundus photos by Reshma et al. methodology into two groups, mild or extreme, according to the number of blemishes observed. Classification of irregular images was 90 percent sensitive. The key downside is that, since the method of removal from retinal pictures of blood vessels by morphological closure with disk structuring factor [53] does not detect mild NPDR, it cannot be used for early detection of DR[43]. Jadhav et al. The DIARETDB photos have been taken into account. The work of Jadhav achieved sensitivity of 90 percent. The function of NPDR and PDR however is not different.

2.4.2 Exudates Detection

Another big DR abnormality is retinal exudates. Thus, the segmentation of bright artifacts in color fundus images was the main focus of many research projects. For example, Reza etc. suggested that the segment algorithm be exuded using methods of image processing based on medium filtering, contrast adaptation, morphology and water-shield transformation [54]. For example. Their exudate segmentation approach achieved 96.7 percent high sensitivity.

In comparaison, Tripathi et al. [55] suggested the latest automated segmentation approach based on the morphologic differential (DMP) profile. The first phase in their work was Gaussian smoothing on the input's green channel, with an increase in contrast. In the DMP the luminous regions that are primarily exudates are observed. The segmentation test exudates achieved 97.63 percent sensitivity. But the precision of their methodologies was not considered in either of the above two studies [55]. Tripathi also worked on STARE pictures that require more techniques for image changes than changing contrasts.

The following three-stage algos have been implemented by Mansour et al. [56]. Discrete Cosine Transform was used for feature extraction including color detail, exudate-segment color histogram threshold and DR SVM. Akter and colleagues [57] suggested an improved method for nonlinear context removal segment exudates. The technique used by Akter et al. would rely on gray images translating from the local thresholds and the median filter to the binary images of loud objects. Erosion and dilation strip the optic disk (OD).

Although 97% sensitivity was reached by the companies of Mansour et al. and 93.55% sensitivity and 99.96% precision by Akter etc., the detection of DR by segmentation of exudates is not successful. But early segmentation of exudates can be used for blindness prevention.

In [58] the authors had established a high gray variation automatic method for segment exudates. Using a clustering technique, the OD has been removed from the image. The SVM was used for the identification of DR severity characteristics of the environment, strength, entropy, smoothness and regions of the exudate. The value of this work is a mild, moderate, extreme NPDR diagnosis. 94.17 percent precision was reached with the classification test. The sensitivity test has not been registered, however. Kuar and Mittal built an algorithm on the other hand[59] based on a modified method of dynamic area cultivation to segments of exudates. 97.9% susceptibility to segmenting exudates has been achieved through their work.

2.4.3 Blood Vessels Detection and Segmentation

The blood vessels and bleeding color are identical, but they vary in size. Many methods for automated segmentation of the retinal blood vessels have also been suggested. Selvathi et al. [60], for instance, suggested a method for Gabor wavelet transform retinal blood vessel segmentation.

In the classification of each pixel by the vessel or non-vessel according to a pixel function vector, SVM and Related Vector Machine (RVM) classificators were used. The downside is the long calculative time for the segmentation of the blood vessels, where the best result was 252 seconds.

Hou [61] introduced a multi-scale blood-vessel-segment detection technique. A linear detector extracts response from the vessels using retinal blood vessel morphological attributes. Each pixel was represented by the vessel. The author has improved a multi-line detector to generate images of vessel response on different scales. As a segmented ship's picture, the line detector with more ship response was considered. These works obtained precision of 93.36 percent. However, Ricci et al. [18] suggested an algorithm based on a lie detector and SVM. However, the sensitiveness was poor at 73.48 percent. They were more exact than Hou reported, 96.46 percent. Pradeep a and Raja [62], by comparison, employed SVM-based approach for the blood vessels section. The Gabor filter and threshold techniques have been used to obtain various characteristics. The work of Pradeepa achieved a precision of 90%. However, sensitivity measurement [62] and [63] have not been reported.

2.4.4 Optic Disc (OD) Detection and Filtering

Yellow on retinal fundus images is the Optic Disc (OD) and exudates. Many algorithms have therefore found and deleted OD to detect exudates more effectively. The OD algorithm based on histogram matches was proposed by Dehghani et al. [64]. As a template for the position of the OD core, the average histogram of each color. For the OD section were used the correlation and thresholding techniques. These works have found the OD perfectly. But only 91.36 percent of the OD pixels can be segmented.

The new OD localization approach focused on the identification of the main vessel as originating from the OD in a similar directional pattern has been proposed by Foracchiaet al. [24]. Then, it proposed geometrical parametric models to define every direction of the retinal vessel and two model parameters were used to detect the OD. This technique is however limited, as only the OD is located.

A method for locating the AD using Circular Hough Transform (CHT) has been proposed by Sekharet al. [25]. As the brightest yellowish circle, the OD was well detected. For position of OD,

CHT demonstrated excellent performance. In [26], an implicit active counter technique was used for the identification of the OD. The OD segmentation results were correct; however, more calculations were required than CHT.

2.4.5 Diabetic Retinopathy Classification

A number of algorithms for classification of DR retinal fundus images have been proposed. For example, Aravind et al. [28] developed a technique for the identification by morphological operations the region, entropy, correlation, energy, contrast, homogeneity and average characteristics have been extracted from the first DR clinical indication microaneurysms. Applied to the classification of the normal NPDR is the vector machine support (SVM), mild or extreme, of each image. Aravind et al. had 92 and 90 percent respectively, for their sensitivity and accuracy. This work benefits from classifying NPDR images into moderate or extreme groups. But moderate NPDR cannot be detected.

On the other hand, the Adaptive Histogram Equalization (AHE) and thresholding detection algorithm are proposed by Sujith Kumar et al. [65]. Each input image is categorized into the regular NPDR or retina. The NPDR images were categorized according to the number of MA identified in groups of mild, moderate or extreme. Unlike Aravind et al., the mild and extreme NPDR were distinguished by Sujith Kumar et al. Sensitivity analysis was not taken into account but the exactness of these tasks was 44.44%.

The key objective of Tjandrasa et al. [66] was to classify NPDR in mild or extreme groups. The exudates were divided into K-means. Three classifications have been used. The multilayer vision, one of the classifiers of the neural networks, has shown the best result in 91.07% accuracy.

2.5 TESTING DATASETS

The proposed approach was tested using three available publicly accessible data sets and a collection of local photographs. A local data system from the Aravind Puducherry Eye Hospital has been tested using the OD Localization Method for both normal and abnormal retinal pictures, including the STARE, DRIVE, MESSIDOR and the OD segmentation.

2.5.1 STARE Dataset

The organized study of the retina (STARE) sub-set includes 81 fundus images which were used for the automatic OD position process by Hoover and Goldbaum (1998). These images were taken with a 35-degree Field-Of-View (FOV) TopCon TRV-50 fundus sensor, which was then digitalized at a 24-bit pixel of 605x700. The dataset includes 31 normal retina images and 50 ill retinas.

2.5.2 DRIVE Dataset

The data set for the DIRVE segmentation of retinal vessels has been developed to promote comparative studies. The set of data contains a total of 40 color fundus pictures, in which no proof of diabetes retinopathy is detected, used for actual clinical diagnoses. 33 pictures. The 24 bits of color pictures from 768 to 584 pixels are comprinted in JPEG format and acquired with a Canon CR5 3CCD 45 FOV non-mydriatic sensor.

2.5.3 MESSIDOR Dataset

In order to simplify the diabetes retinopathy computer-assisted diagnose studies, methods for testing segmentation and indexing techniques have now been developed in the field of retinal ophthalmology (MESSIDOR). 3 ophthalmological departments used a 3CCD color video camera for Topcon TRC nw6 non-mydriatic retinography, with 45 degree view, created the 1 200 color fundus numeric images of the back pylon of the MESSIDOR database. The photos were taken with 8 bits in 1440 * 960, 2240 * 1488 or 2304 * 1536 pixels per color plane. Some 800 pictures with dilation and 400 without dilation have been obtained.

2.5.4 LOCAL Dataset

Aravind Eye Hospital in Puduchery has obtained a total of 100 retinal photographs. There are 50 normal retinal and 50 abnormal fundus photos. The data are being collected. The number of patients aged 30-70 was approximately the same for men and women. All was taken with a 30-degree Field-Of-View (FOV) image format 2196 X 1958 pixels. Eye experts mark the optical disk and cup. Three specialists with various clinical backgrounds of 3, 8 and 15 years respectively

gathered simple facts. The reality is that cup bounds and cup-to-disk (CDR) values are the base. Each picture had two diagnoses: DR grade and macular edema risk.

Retinopathy consists of four degrees. Grade 0 applies to non-retinopathy, Grade 1 and Grade 2 to NPDR, Grade 3 to Severe NPDR or Proliferative Retinopathy (PDR) patients. NPDR is category 0. There are three steps of the probability of macular edema. Grade 1 is the same as the fovea exudate images larger than 1 disk of diameter, and grade 2, which is the equivalent of fovea exudate images in 1 fovea disc.

2.5.5 Summary of Database

As shown in Table 2.1, the database used for OD localization is. For automated localization and OD segmentation, a collection of 1421 retinal images is thus checked..

Table 2.1: Database used for OD localization and segmentation

S.No	Dataset	Total images	Normal images	Diseased images
1	STARE	81	31	50
2	DRIVE	40	33	7
3	MESSIDOR	1200	546	654
4	Local	100	50	50
	Total	**1421**	**660**	**761**

2.6 CONCLUSION

There are 5 chapters in the study. This chapter includes context information and a literature review to detect and classify DR automatically. Furthermore, we are explaining the difficulties and significant details about DR.

3. METHODOLOGY

Various methods for optical disk detection and segmentation are available in the literature. The OD segmentation technique proposed by Fraga et al. in various stages [4]. The retinal image algorithm was normalized in [5] using the retinal image, which decreased contrast variability and improved process efficiency. Many such algorithms detect the optical disk, but the algorithm proposed here is easy and faster to implement.

The border of the optical disks is located in the proposed work in three phases. Next, blood vessel segmentation is done from the color picture of the retina. Next step is to find where blood vessels come from which the segmented blood vessels can be divided into image blocks and the amount of non-zero pixels calculated in a block can be calculated. The maximum non-zero-pixel block marks the origin position of the blood vessels. Use it to locate the optical disk center after the block is located. Segment the optical disk on the center and trace a circle by means of the center;

3.1 PROPOSED SYSTEM OVERVIEW

In this review, we propose a new method for detects OD boundaries more accurately and with a low computational complexity than the literature. The flowcharter shown in Figure 3.1 summarize our proposed OD boundary detection algorithm.

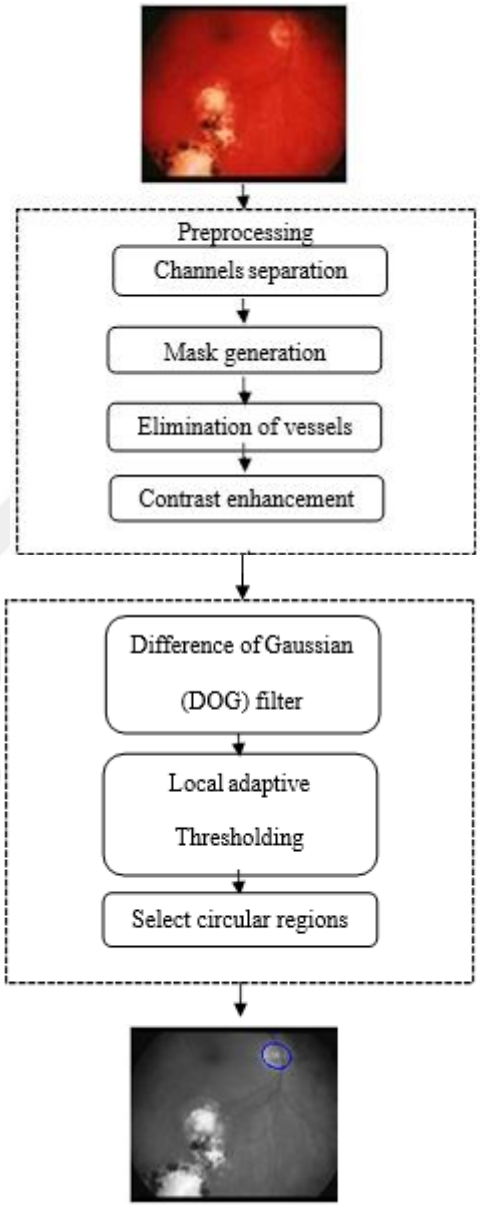

Figure 3.1: Flow chart of the proposed algorithm

3.1.1 Preprocessing step

There are four subphases of the preparation stage, the first being the channel separation. Three different channels reflect retinal color (RGB): red, green and blue. (Table 3.2). This is the red channel, and the OD is in shape 1. The green channel [17] is the highest contrast, and the blue channel is very dark and sounds a lot. In OD detection, most research uses the green channel [9],

but in some cases it appears that the red channel is a better alternative. In this article, we use the two parallel channels to boost the detection algorithm 's efficiency Further increases the retinal image to 0.5, which decreases the costs of measurement without affecting the efficiency of the algorithm by sampling to 0.5 its original dimension. In the following sections, the other three steps are listed.

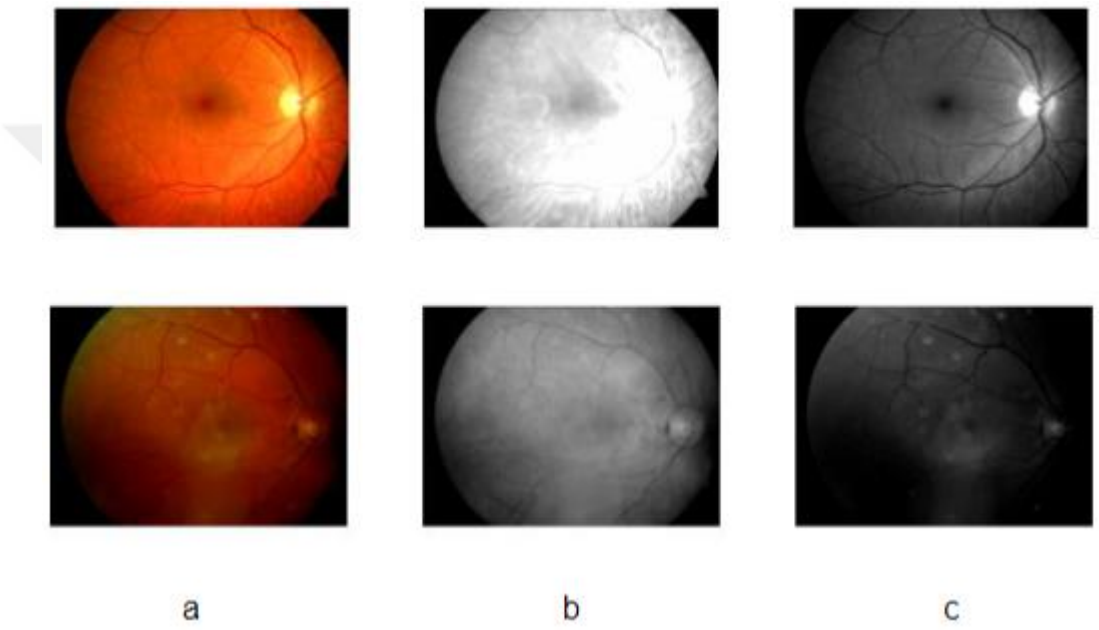

Figure 3.2: Retinal color pictures: (a)RGB image, (b) red channel, and (c).

3.1.2 Mask generation.

A binary mask is used to avoid further processing of background pixels. The mask is generated in [18] in which the red channel from the original RGB image was extracted and thresholded into a binary image. The same kernel (3x3 square kernel) was then used for morphological opening, closing and then erosion.

3.1.3 Elimination of vessels.

Blood vessel presence makes it impossible to reliably detect OD boundary, Thus, with morphological procedures, blood vessels have been eliminated. Only smaller details than the structural element used are removed by the closure of the image and it is defined as the dilation, then erosion, given by (3.1):

$$I \cdot S = (I \oplus S) \ominus S \qquad (3.1)$$

Where I and S are respectively a picture and the structuring part. Dilation and erosion in (3.2,3.3) pixels (x, y) shall be identified.:

$$(I \oplus S)(x, y) = max_{i,j}[I(x - i, y - j) + S(i, j)] \qquad (3.2)$$

$$(I \ominus S)(x, y) = min_{i,j}[I(x + i, y + j) - S[i, j] \qquad (3.3)$$

Where I and j are indexing S pixels. Based on the blood vessels, the size and type of the structuring factor. The vessel is commonly believed to not be larger than 15 pixels, so that a 15x15 symmetrical structural feature is used in the form of a disk.

3.1.4 Contrast enhancement.

Low retinal image contrast makes it harder to display OD, and we must therefore increase the contrast of this image. The contrast can be increased or decreased with Gamma Transformations. In this case the difference between the input and the output image is increased (gamma is less than one) by [19] in (3.4):

$$O = cr^{\gamma} \qquad (3.4)$$

Where o is the image of output, r will be the picture of input, c positive, and μ the gamma value. Figure 3.3 shows this pre-processing phase.

Figure 3.3: (a) sub-image, (b) closing, (c) enhancing contrast;

3.1.5 Extraction of circular regions

3.1.5.1 Difference of Gaussian (DOG) filter

The OD is more or less circular in shape, but because of its shape it is also an ellipse. After eliminating blood vessels and enhancing contrast, OD and center is detected with a gaussian differences (DOG) filter.

In the beginning, the Gaussian function G1 of retinal input image I had a width¨1 for obtaining L1. (3.5) The gauze function G is shown:

$$G(X,Y,\delta) = \frac{1}{2\pi\sigma^2} exp^{-\frac{x^2+y^2}{2\sigma^2}} \quad (3.5)$$

This fluttered L1 image is transformed into a second L2 image by means of a Gaussian G2, width σ^2, in which¨2= k¨1 (k=2, as calculated experimentally in the present study). The L1-L2 difference is then evaluated according to the description of (3.6):

$$D(X,Y,\sigma) = (G(X,Y,k\sigma) - G(X,Y,\sigma)) * I(X,Y) \quad (3.6)$$

Where * is the x and y operation of the convolution. For a binary radius circle, as stated in [28] r, the filter achieves a maximum at (3.7):

$$\sigma = \frac{r}{\sqrt{2}} \quad (3.7)$$

In our experiments r represents the approximated radius of the OD, which is calculated according to8,where the OD occupies about one-seventh of the entire image.

3.1.5.2 Local adaptive thresholding

Two key types of threshold methods are global and local thresholds. The threshold value is constant in global thresholds, leading to inaccurate results for inaccurate lighting. In comparison, in the local threshold, the threshold value varies to compensate for the uneven lighting behind the scenes. This can be done by the use of local pixel29 information by the individual measurement of retinal background thresholds for each pixel. Because of uneven light images, an adaptive local threshold is used.

In this thesis, the savage technique was used since, by means of m(x, y) and standard variation (x , y) mean values of each pixel in the particular image is calculated by the use of a given pixel(x, y) centered around pixel(x, y) pixel(3.8). The thesis is also marginally better than the technology of Otsu [30]:

$$t(x,y) = m(x,y)\left[1 + q\left(\frac{s(x,y)}{R} - 1\right)\right] \quad (3.8)$$

The value R is the maximum default value (R=128), and the value q is the product (in this study q= 0.3430). The results are shown in Fig. 4 (Binary image of many subjects).

The item is finally chosen which is more circular than a preset value; in Figure 3.4 the results are shown. This step is shown. Figure 3.4 shows the method for the approximation of the OD circular limit measurement.

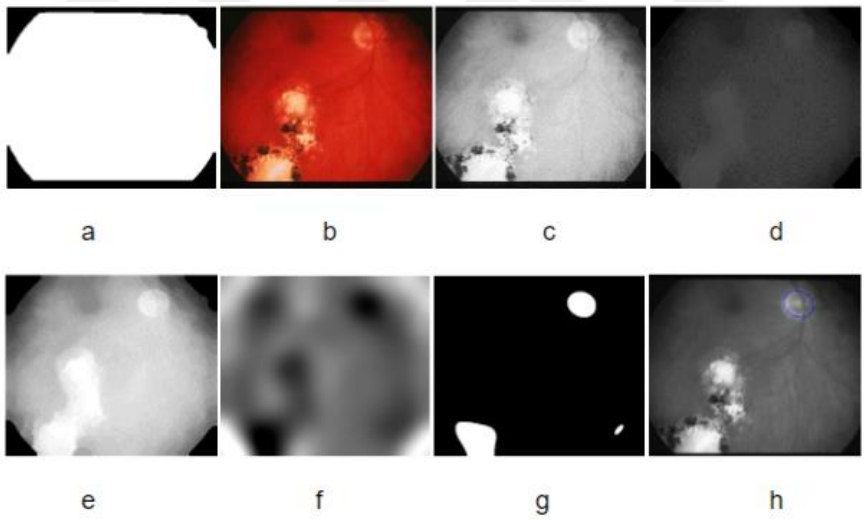

Figure 3.4: b)RBG image input, c) channel chosen, d) closing, e), enhanced setup, f) DOG filter, g) thresholding and h) Bounding approximation circular OD boundary.

3.2 RESULTS AND PERFORMANCE ANALYSIS

In this research work, a MATLAB directional matching filer (R2013a) has introduced the proposed OD localization method where average running times of 25 seconds Are asked (Pentium(R) Dual-Core2 and T4300@2.10GHz, 3.00 GB RAM 64-bit OS) for any image on your laptop.

The OD localization approach was tested using the STARE, DRIVE, MESSIDOR and the local data collection from the Aravind eye hospital Puducherry for both normal and abnormal images. Figure 3.10 to Figure 3.11 shows a representative retinal image from STARE, DRIVE, MESSIDOR and local dataset.

In Figures 3.10 and 3.11 all representative retinal images show different lighting, independent of normal or pathological condition. The lighting changes play a major role in influencing the detection 's performance. In order to avoid uneven lighting (background normalized) within the images the images are subject to average filter compensation technology.

A disk-based binary template from the background normalized image was used to find the OD candidates. Figure 3.12 to 3.13 show the detected OD location. The findings were obtained based on the original image resolution in this study. Results of OD detection. If it is within the OD range of the reference standard the detected OD-center is considered a successful detection. The OD candidate in the region following matched filtration is to be determined as OD location for representative images of the retinal, as shown in Figures 3.13 to 3.16.

3.2.1 Datasets

The dataset31 of the STARE is composed of 81funds of the dimensions 605 to 700 (31 regular and 50 diseased). Figure 5 displays random samples from the STARE data set to demonstrate the identification of the OD boundary. The approach proposed allows for the segmentation of 80 images out of 81 images with a 98.8% success rate, the highest result for the results recorded in table 3.1. The results recorded for [9] were obtained from the STARE dataset on 17 images out of 20 images. In addition, for10 findings were obtained in 18 of only 20 photographs.

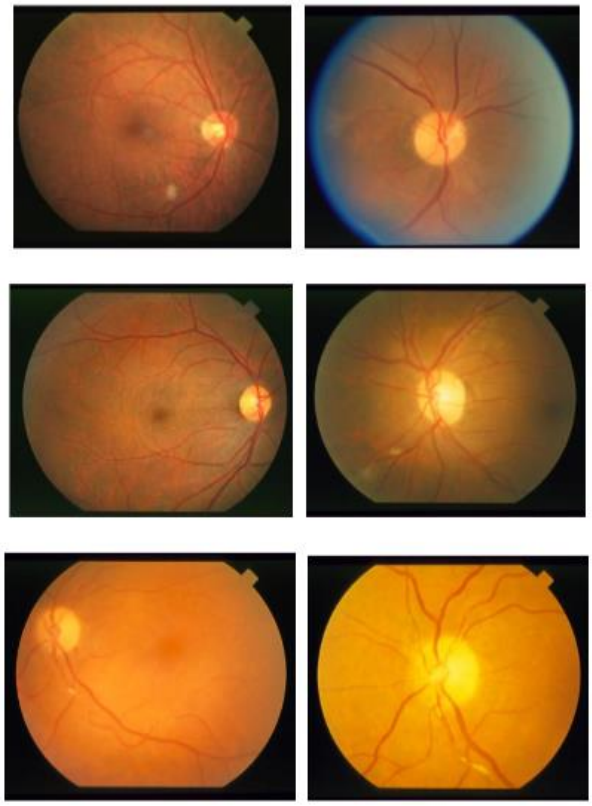

Figure 3.5: Representative retinal images from STARE dataset

The DRIVE data set comprises 40 fundus images, measuring 584 daily to 5565 (33 normal and 7 disease) and is focused on retinal frames [32]. Our method proposed is capable in all 40 images of properly detecting the OD boundary. The rate of success was 100%. This is stronger than in [9] as seen in Table 3.2. Figure 3.11 shows the results for sample images from this database.

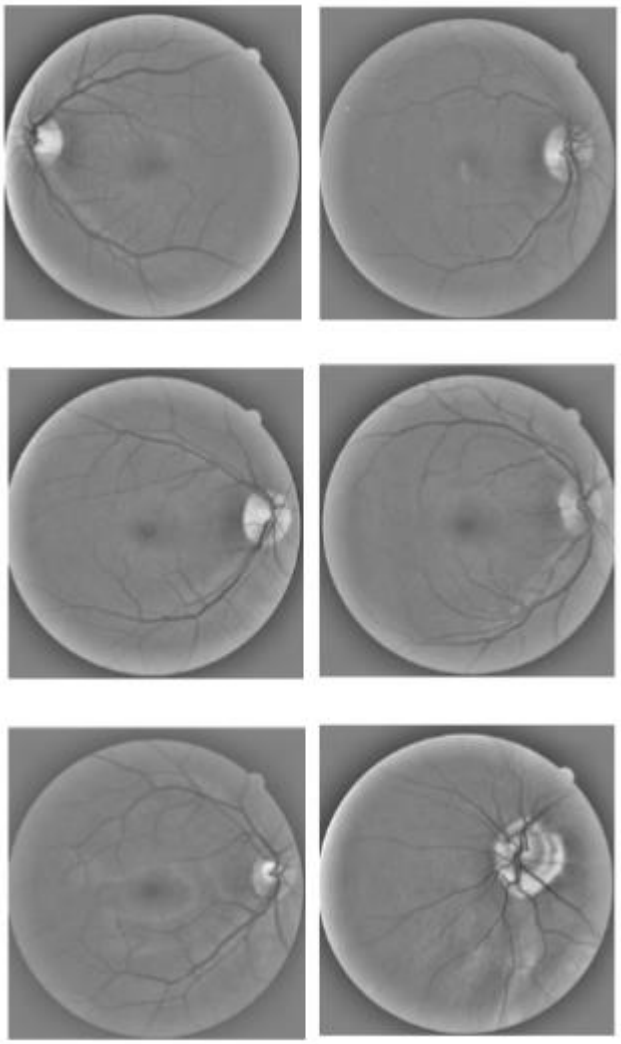

Figure 3.6: Background normalized image from DRIVE dataset

ARIA dataset: contains 120 fundus pictures (59 diabetes pictures and 61 control pictures) of the 576 dimensions of 0.44 sec and a performance rate of 100% compared to 97.5% in +16. Figure 3.12 shows random samples from the dataset. The green border reflects the truth of the floor, while our area is blue. Experts have manually marked the ODs to reveal the fundamental truth of the detection in this dataset. The accuracy of this set of data (3.9) is calculated:

$$Accuracy = \frac{(TP+TN)}{(TP+FN+TN+FP)} \times 100 \qquad (3.9)$$

where:

True positive (TP): Right classification of OD pixels as OD pixels.

False positive (FN): Pixels that are not OD misclassified as area of OD.

True negative (TN): The correctly defined non-OD pixels to non-OD pixels.

False negative (FP): Misclassified OD pixels as non-OD pixels

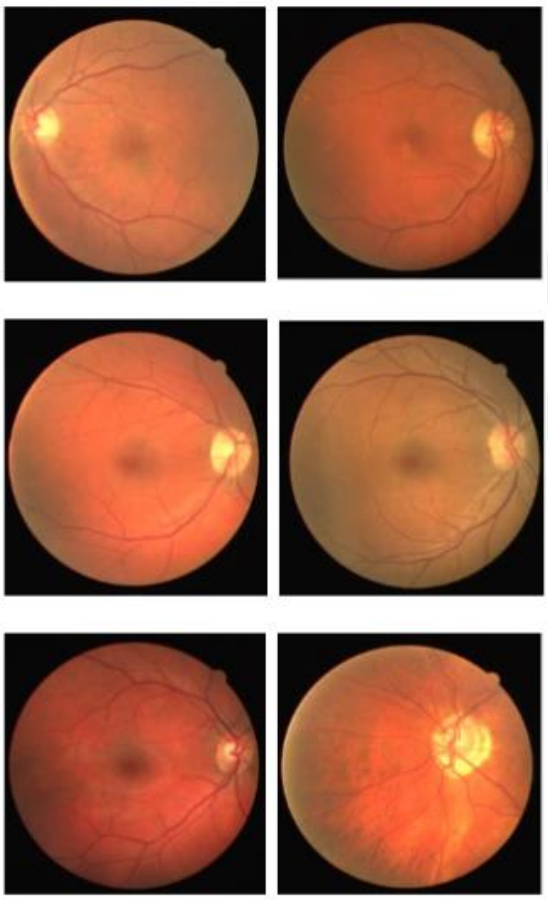

Figure 3.7: Representative retinal images from DRIVE dataset

DIARETDB1 contains 89 fundus images of the sizes 1152 da1500 (5 ordinary) and 84 illnesses (84 illnesses) and DIARE TDB0 dataset 34 of the sized measurements 1152 da1500 (20 usual and 110 illnesses). The results reported for DIARETDB1 and DIARETDB0 were 97.8 and 98.5%, as illustrated in Table 3.4, respectively. Figure 3.13 shows the findings for sample images from these databases.

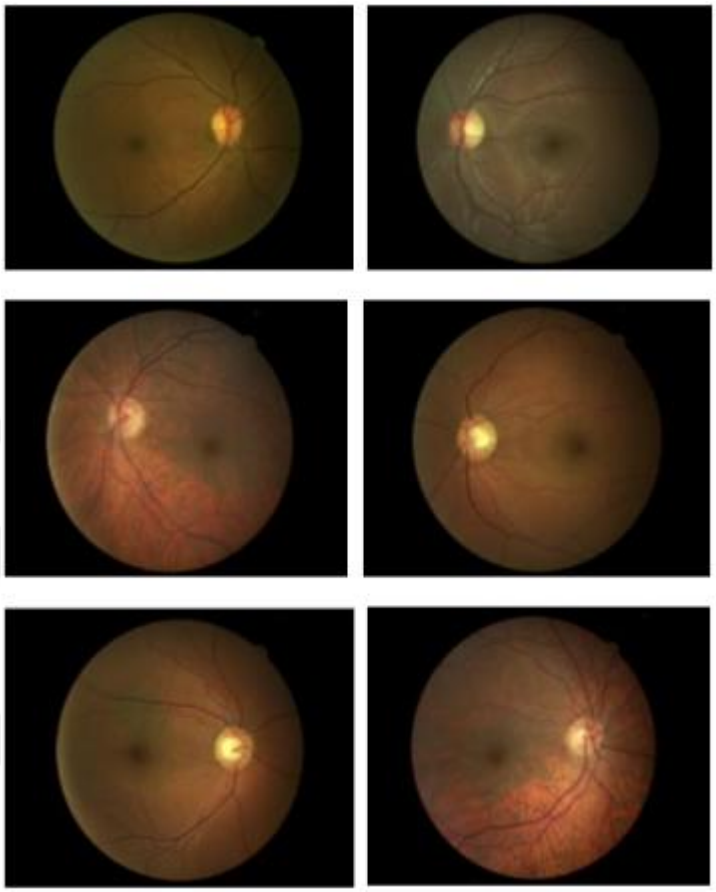

Figure 3.8: Representative retinal images from DIARETDB1

The dataset for MESSIDOR consists of 1200 color fundus pictures collected from 3 aphtha's. Photographs were taken with 8 bits of 1440 – TO 960, or 2240 – TO 1488, or 2304–1536 pixels per color plane. As compared with 99% and 99,70% of the work listed in Table 4, according to Table 3,3, our approach has achieved a success rate of 99,83%.

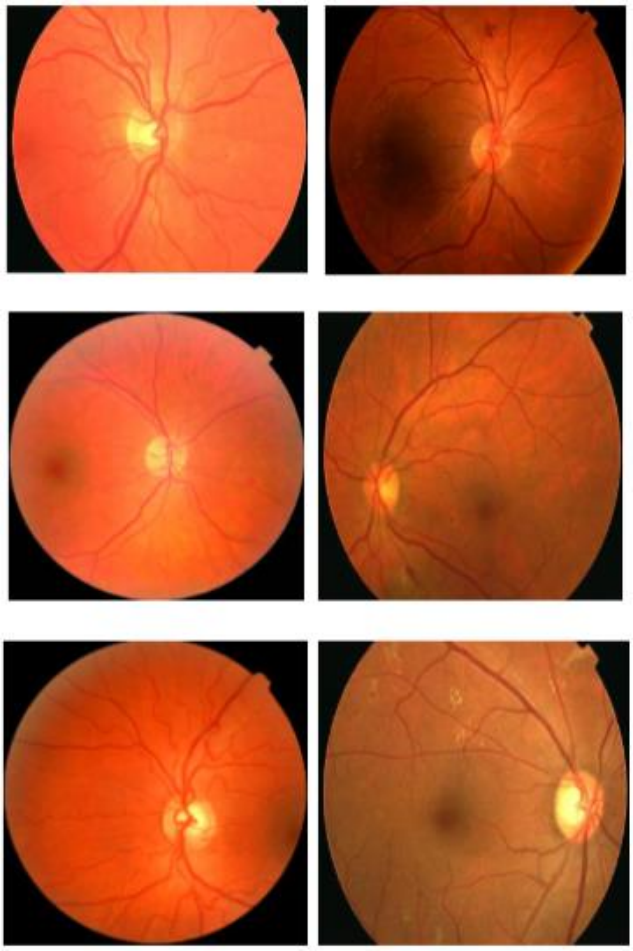

Figure 3.9: Representative retinal images from MESSIDOR dataset

Table 3.1: Comparison of OD detection methods STARE dataset

Method	Success Rate	Computational Time
[8]	42.0%	NA
[9]	82.3%	NA
[10]	90%	NA
[11]	91.36%	32.5 sec
[12]	71.6%	1.6 sec
[13]	97.5	2 min
[15]	89.0%	15 sec
[16]	98.77%	5 sec
[17]	92.6%	0.46 sec
[18]	98.8%	3.5 min
Proposed	98.8%	0.45 sec

[a] The success rates and the computation times are taken from [18]

[b] The success rates and the computation times are taken from their corresponding references.

Table 3.2: Comparison of DRIVE Dataset OD detection methods.

Method	Success Rate	Computational Time
[9]	90%	NA
[10]	100%	NA
[11]	100%	27.6 sec
[18]	100%	0.32 sec
[21]	100%	2.1 min
Proposed	100%	0.36 sec

[a] The success rates and the computation times shown are taken from corresponding.

[b] The success rates and the computation time is taken from Dehghani et al. [11].

Table 3.3: Comparison of OD detection methods MESSIDOR dataset

Method	Success Rate	Computational Time
[4]	99%	5.69sec
[16]	99.75%	NA
Proposed	99.83%	3.1 sec

Table 3.4: DIARETDB1 and DIARETDB0 datasets comparison of OD detection methods.

Method	DIARETDB1		DIARETDB0	
	Success Rate	Computational Time	Success Rate	Computational Time
[18]	97.8%	0.98 sec	98.5%	0.98 sec
Proposed	100%	1.5 sec	100%	1.5 sec

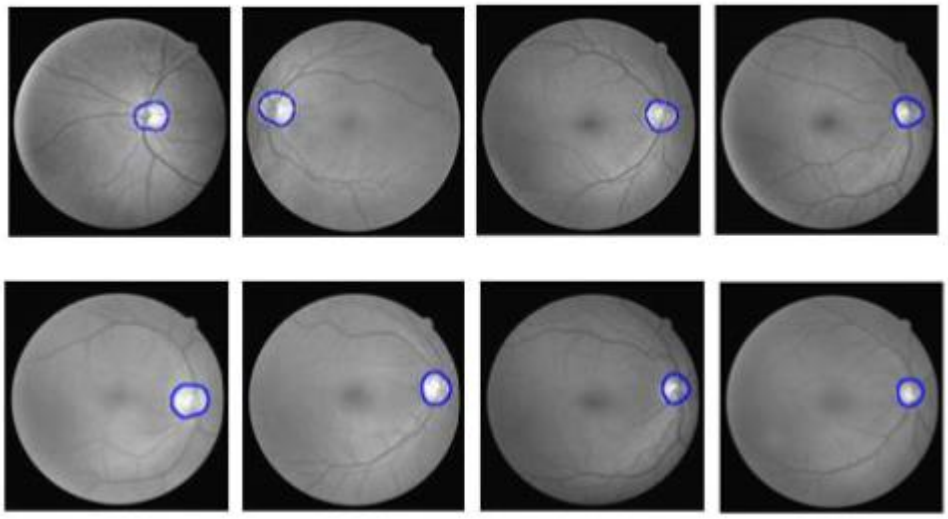

Figure 3.10: Results for STARE dataset random samples.

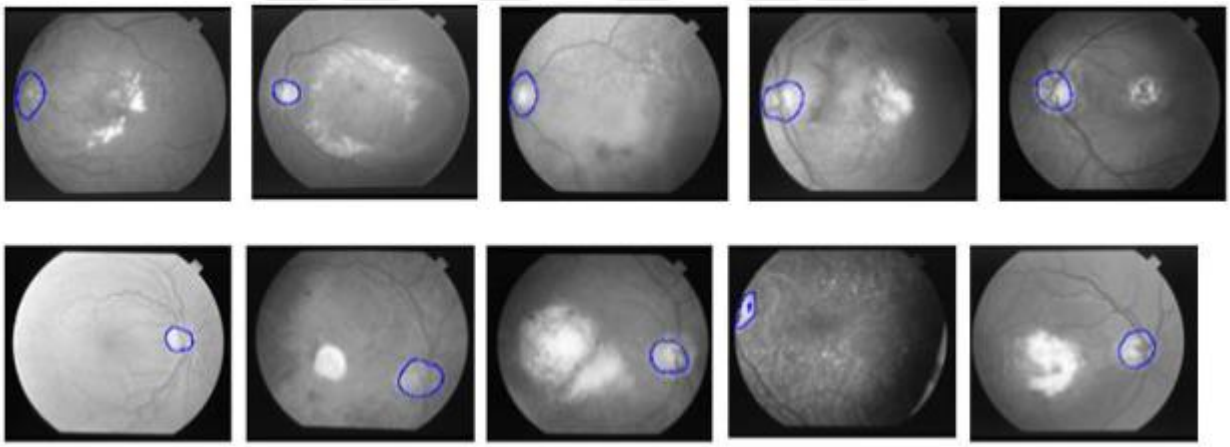

Figure 3.11: Random DRIVE dataset sample outcomes.

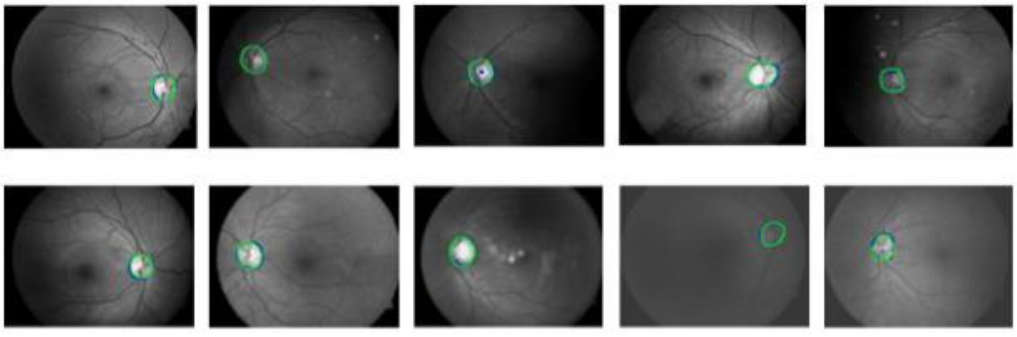

Figure 3.12: Results for random samples from ARIA dataset (blue) and the ground truth in green.

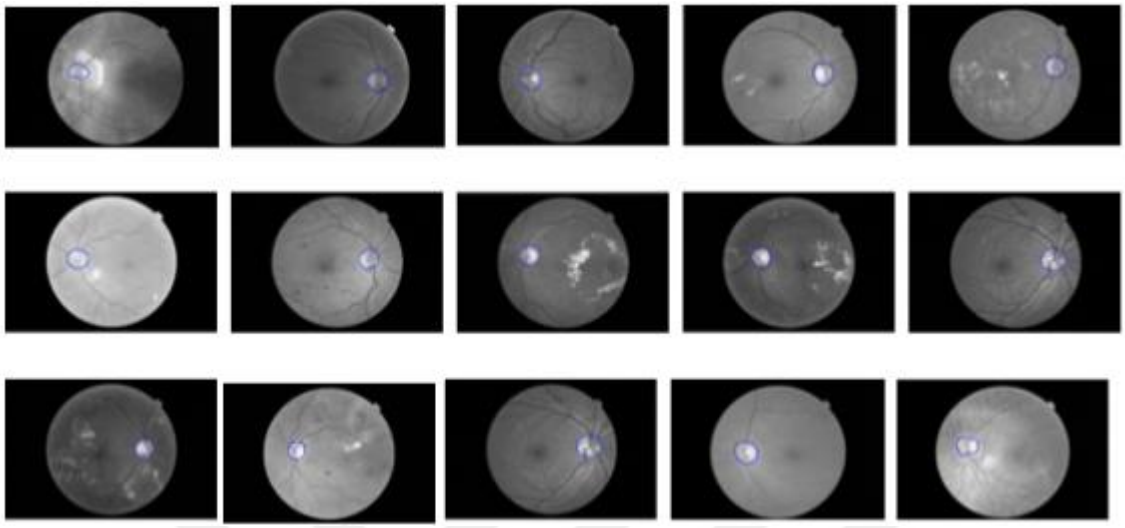

Figure 3.13: DIARETDB1 (up) and DIARETDB0 (down) data collection Random sample results.

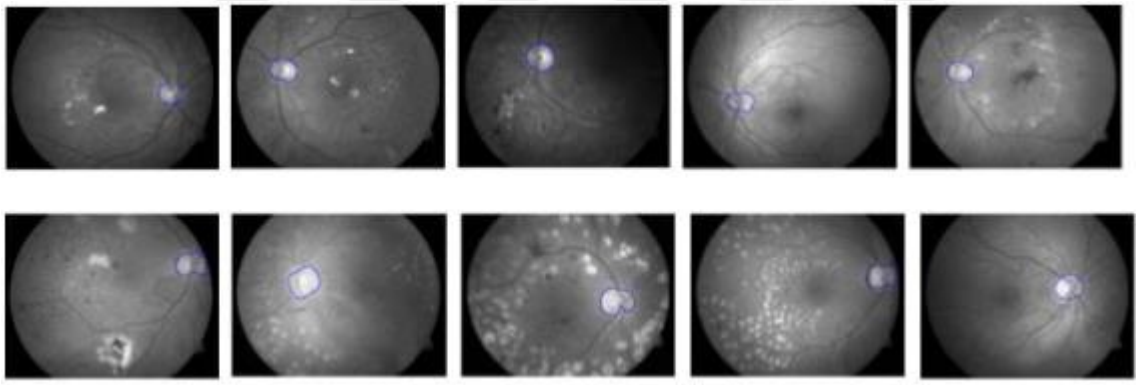

Figure 3.14: Results for random samples from MESSIDOR dataset.

3.2.2 Robustness of OD Localization Methodology

The bright images, (2) light images and (3) pathologically arranged images are based on their OD location output (1), the robustness of the proposed methodology is assessed. Three types of sounds usually used in biomedicine images (Gaussian, Salt & Pepper and Speckle Noise) corrupt the retinal images. Figure 3.15, 3.16, 3.17 shows that, while the retinal images were deteriorating markedly due to additional noise, OD is successfully identified. The second measurement criterion is OD 's assessment against contrast and lighting which makes OD's detection difficult because the OD's in the background is obscured with poor contrast and illumination. Figure 3.18, 3.19 indicates

some extreme cases where the proposed approach effectively localizes OD and bad contrast and illumination.

Increased segmentation of the optical disks is threatened by pathologies such as papillary atrophy, fungi and lesions because certain diseases may occur bright or circled and it may lead to misclassification.

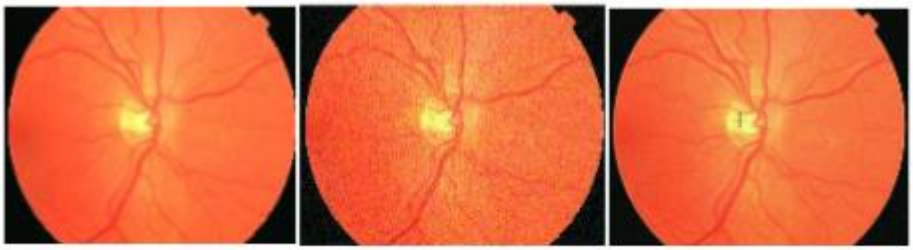

Figure 3.15: Gaussian noise performance (a) Original picture (b) Noisy picture (c) OD detection.

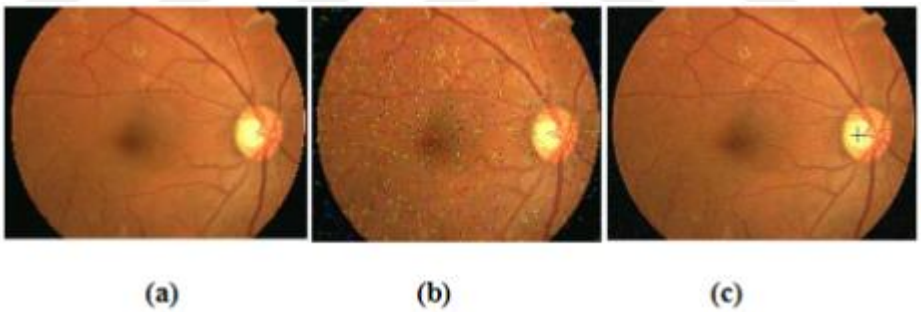

Figure 3.16: Performance in pictures of salt and pepper noise (a) Initial (b) noisy (c) OD.

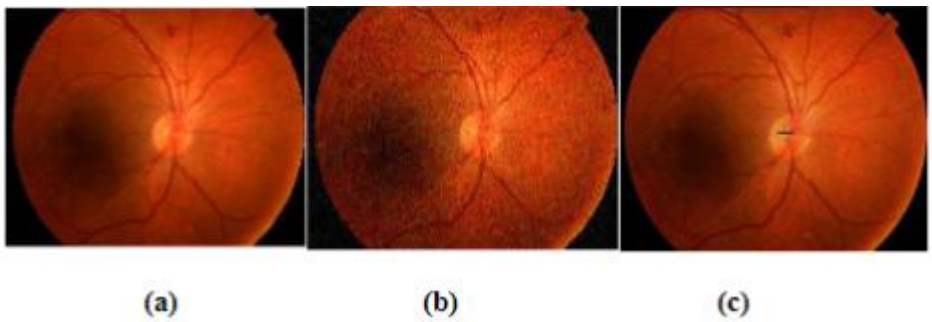

Figure 3.17: Noisy photo detection (c) OD image (a) Initial pictorial photo (b).

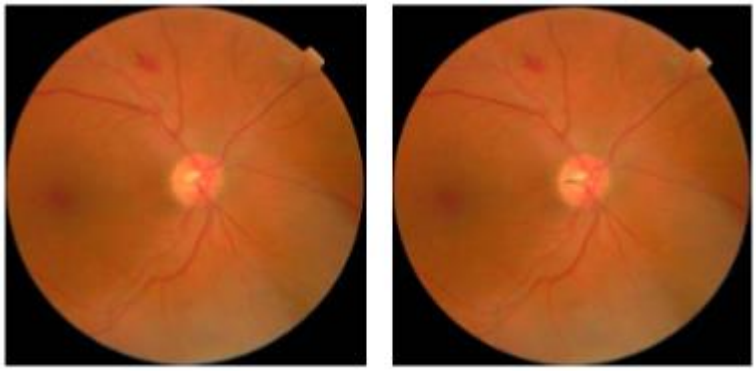

(a) (b)

Figure 3.18: Lack of contrast efficiency (a) initial OD detection image (b).

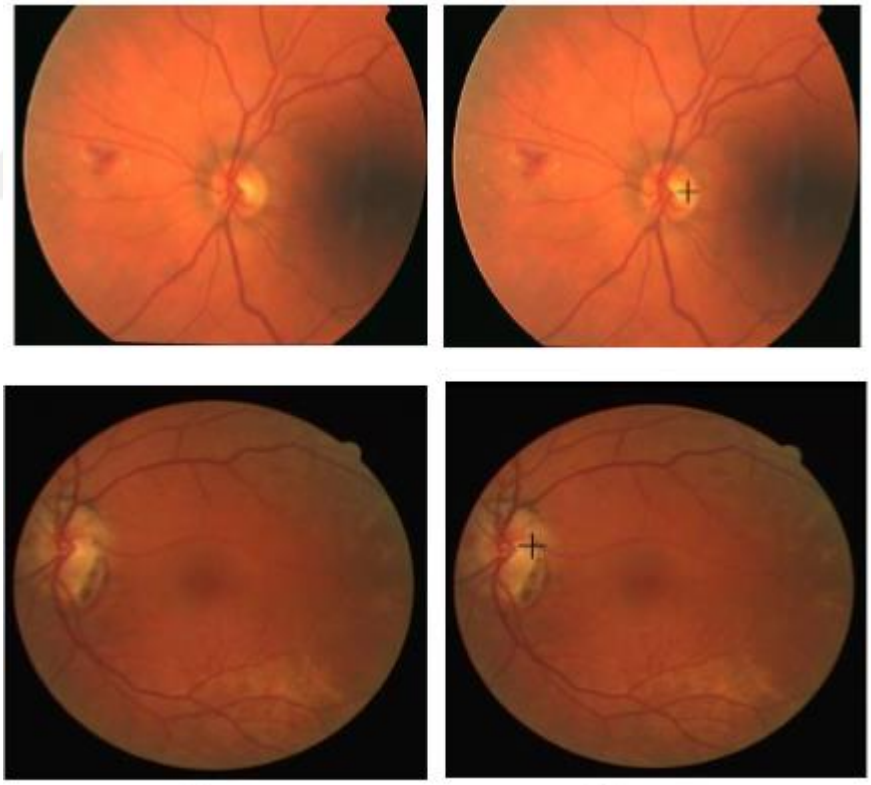

(a) (b)

Figure 3.19: Uniform illumination efficiency (a) OD detection original image (b).

The OD detection was performed on four retinal image data sets such as STARE, DRIVE, MESSIDOR and local datasets with the help of a matched directional filter. Experimental evaluation reveals that in the processing process the technique works easily, robustly to differences in image contrast and lighting.

The power of the OD detection and segmentation has been assessed based on the noisy images with lighting devices and images with pathological structures. Despite a substantial deterioration in retinal images, the technique effectively segmented the OD. In addition, the algorithms work well with the images and pathological structures with uneven illumination.

3.3 DISCUSSION

A series of 1660 colored retinal images from six publicly available data sets were used in our experiments. To detect the OD limit, the method proposed is used. This gives the algorithm an excellent opportunity to test images with various characteristics; normal, anomalous, different dimensions and imagery methods.

The CPU is a 3.30 GHz Inter(R) core (TM) i3-3220 CDU and a 2 GB PC RAM algorithm with MATLAB. The results demonstrate that both the success rate and computing time of the proposed method perform better than the literature methods published. In addition, ARIA and MESSIDOR datasets were not checked for this method18. Our method was the first to use and publish the findings of all six datasets based on the literature method. Further research to minimize calculation time will be performed.

The proposed technique is evaluated for performance evaluation using six available datasets, the STARE31, DRIvE32, ARIA33, Standard Diabetic Retinopathy Databases 34 "Level 1 calibration" (DIARETDB1) and the "Calibration Level 0" (DIARETDB0) and MESSIDOR35 standard Diabetic Retinopathy database.

3.4 CONCLUSION

This study proposes a new algorithm to detect the OD border, obtained via morphology and contrast increases, then apply the DOG filter using two OD-radius sigma values, threshing and choosing circular object areas the following sigma values. This analysis is also available in the following report. The first to be checked with the 6 publicly accessible databases is the algorithm proposed. Experimental findings indicate good performance with an reasonable processing time compared to literature methods.

4. CONCLUSIONS AND FUTURE WORK

4.1 CONCLUSIONS

The primary step in designing automated screening systems is optical disk segmentation. The specificity of the segmentation approach helps to accurately classify pathologies such as diabetic retinopathy and glaucoma. Similarly, the first step in segmentation is optical disc detection, which will lead to promising results for segmentation.

This thesis presents a method for an automatically matched filter and operator scission for automatic optical disk identification and segmentation of retinal images. The first key step in retinal image processing is optical disk detection.

Four retinal image datasets including STARE, Move, MESSIDOR, and local datasets have been analyzed using the OD detection process. Experimental assessments indicate that this approach is easy to calculate, the contrast and illumination variance is stable, works well in pathological retinal images and is comparable in quantitative performance measurements to state-of-the-art methodologies. The methodology provides 97% of OD detection in STARE, 100% for DRIVE, 99% for MESSIDOR, and 96% for local datasets.

OD detection and segmentation findings clearly demonstrate the ability to segment the system proposed even when the OD limits are uncertain, and where there are pathologies such as atrophy of papilla that raise the risk of false positives. Based on the OD position and segmentation (1) of the noisy photos, (2) of the illuminated images and (3), the robustness of the proposed technique was evaluated. The retinal pictures were distorted for evaluation with three different forms of noise, In the biomedical pictures, commonly found are gaussian, bacon noise and salt and pepper. Despite substantial degradation of the retinal images, the technique effectively segmented the OD. Moreover, the photos of unequal illumination, pathological structures and algorithms work well.

On local dataset, the OD segmentation approach has been tested. Compared to others state-of- the art approaches, the proposed approach achieved improved operating characteristics for recipients (ROC), quantitative analyzes and Cup to disk ratio.

For the following applications, an automated process is also useful.

- Retinal anatomy localization and segmentation, including blood vessels, macula, fovea, and the anatomic anatomy of other organisms such as microaneurysms, bleeding, and drusen exudates.
- In macular retinal images, to distinguish the left and right eyes.
- Position of OD is a first crucial move for automated analysis of retinal images.
- OD was also used to map the retinal vasculature as an initial stage. The proposed automated system thus assists in the diabetic retinopathy, glaucoma and other eye conditions screening process.

4.2 FUTURE WORK

Its power, in particular for difficult images, is the advantage of the proposed process. The lighting image and the retinal image with pathological changes contain these challenging images.

In the future the proposed method could be evaluated for other massive, accessible and publicly available datasets An extension of this study could be the following:

- Improvement of ship segmentation algorithm output, which would dramatically impact the proposed method's performance and quality. This can be accomplished by transforming the wavelet.
- To boost the efficiency of the OD center by using fractals to remove the blood vessels.

REFERENCES

[1] Maninis, KK, Jordi, PT, Pablo, A & Luc, VG 2016, "Deep Retinal Image Understanding", International Conference on Medical Image Computing and Computer-Assisted Intervention. Springer International Publishing, pp. 140-148

[2] Tagore, MRN, Krishna, REV & Prabhakar, RB, 2016, "An Accurate Optic Disc Segmentation from Peripapillary Atrophy Incident Retinal Images", International Journal of Computer Applications, vol. 147, no. 11, pp. 14-20

[3] Sengar, N, Kishore, MD, Parthasarathi, M, Sohini, R & Radim, B 2016, "Fast localization of the optic disc in fundus images using region-based segmentation", Proceeding of International Conference on Signal Processing and Integrated Networks, pp. 529-532.

[4] Sharma, A & Shaveta, R 2016, "An automatic segmentation and detection of blood vessels and optic disc in retinal images", Proceeding of International Conference on Communication and Signal Processing,pp. 1674-1678

[5] Goran & Alistair 2011, "Anatomy and physiology of retina", Pediatric Retina, Springer, pp. 39-65.

[6] Melinda, YC, Stacy, L & Pineles 2016, "Optic disk drusen in children", Survey of Ophthalmology, vol. 61, no. 6, pp. 745–758.

[7] Angel Suero, Diego, M, Manuel, EGA & Jose MB 2013, "Locating the Optic Disc in Retinal Images Using Morphological Techniques", Proceedings of IWBBIO.

[8] Yu, H, Barriga, ES, Agurto, C, Echegaray, S, Pattichis, MS, Bauman, W & Soliz, P 2012, "Fast Localization and Segmentation of Optic Disk in Retinal Images Using Directional Matched Filtering and Level Sets", IEEE Transactions on Information Technology in Biomedicine, vol. 16, no. 4, pp. 644-657.

[9] Jonas, JB, Wang, N, Yang, D, Ritch, R & Panda, JS 2015, "Facts and myths of cerebrospinal fluid pressure for the physiology of the eye", Progress in retinal and eye research, vol. 46, no. 1, pp. 67-83.

[10] Jonas, JB, Wang, N, Yang, D, Ritch, R & Panda, JS 2015, "Facts and myths of cerebrospinal fluid pressure for the physiology of the eye", Progress in retinal and eye research, vol. 46, no. 1, pp. 67-83.

[11] Sandro, IDZ, Carlos, C, Tobias, R, Philippe, M, Francis, M, Aubin, B, Meritxell, BC & Jens, HK 2015, "Landmark Detection for Fusion of Fundus and MRI Toward a Patient-Specific Multimodal Eye Model", IEEE tran.on Biomedical Engg., vol. 62, no. 2, pp. 532-540.

[12] Sengar, N, Kishore, MD, Parthasarathi, M, Sohini, R & Radim, B 2016, "Fast localization of the optic disc in fundus images using region-based segmentation", Proceeding of International Conference on Signal Processing and Integrated Networks, pp. 529-532.

[13] Yang, Z, Tatham, AJ, Zangwill, LM, Weinreb, RN, Zhang, C & Medeiros, FA 2015, "Diagnostic ability of retinal nerve fiber layer imaging by swept-source optical coherence tomography in glaucoma", American journal of ophthalmology, vol. 159, no. 1, pp. 193-201.

[14] Singh, A, Dutta, MK, Parthasarathi, M, Uher, V & Burget, R 2016, "Image processing based automatic diagnosis of glaucoma using wavelet features of segmented optic disc from fundus image", Computer methods and programs in biomedicine, vol. 124, no. 1, pp. 108-120.

[15] Sudeshna, SK & Santi, PM 2016, "Blood vessel extraction and optic disc removal using curvelet transform and kernel fuzzy c-means", Computers in Biology and Medicine, vol. 70, no. 1, pp. 174–189.

[16] Kittipol, W, Nualsawat, H & Ekkarat, P 2014, "Automatic Detection of Optic Disc in Digital Retinal Images", International Journal of Computer Applications, vol. 90, no. 5, pp. 15-20.

[17] Sinha, N & Babu, RV 2012, "Optic disk localization using L1 minimization", Proc.of IEEE International Conference on Image Processing, pp. 2829-2832.

[18] Zhang, Z, Yin, FS, Liu, J, Wong, WK, Tan, NM, Lee, BH, Cheng, J & Wong, TY 2010, "ORIGA (light): an online retinal fundus image database

for glaucoma analysis and research", Proc. IEEE Eng. Med. Biol. Soc., Buenos Aires, pp. 3065-3068.

[19] Li, HLH & Chutatape, O 2001, "Automatic location of optic disk in retinal images", Proceedings of International Conference on Image Processing, vol. 2, pp. 837–840.

[20] Li Xiong & Huiqi Li 2016, "An approach to locate optic disc in retinal images with pathological changes", Computerized Medical Imaging and Graphics, vol. 47, pp. 40–50.

[21] Kemal, A, Baha Fen & Fafak Bayir 2016, "Automatic Detection of Optic Disc in Retinal Image by Using Keypoint Detection, Texture Analysis,and Visual Dictionary Techniques", Computational and Mathematical Methods in Medicine, vol. 2016, pp. 1-10.

[22] Avinash, R & Venkatesh, R 2014, "Approximate Nearest Neighbour Field based Optic Disk Detection", Computerized Medical Imaging and Graphics, vol. 38, no. 1, pp. 49–56.

[23] Joshi, GD, Gautam, R, Sivaswamy, J & Krishnadas, SR 2010a, "Robust optic disk segmentation from colour retinal images", Proceedings of the Seventh Indian Conference on Computer Vision, Graphics and Image Processing, pp. 330-336.

[24] Jun Cheng, Dacheng, T, Jiang, L, Damon WKW, Ngan, MT, Tien YW & Seang, MS 2012, "Peripapillary Atrophy Detection by Sparse Biologically Inspired Feature Manifold", IEEE Transactions on Medical Imaging, vol. 31, no. 12, pp. 2355-2365.

[25] Ana, SG, Djibrilkaba, YL & Liu X 2014, "Segmentation of blood vessels and optic disc in retinal images", IEEE Journal of Biomedical and health informatics, vol. 18, no. 6, pp. 1874-1886.

[26] Arriagaa, JA, Edgardo, M, Felipe, R & Eduardo GC 2014, "Application of vascular bundle displacement in the optic disc for glaucoma detection using fundus images", Computers in Biology and Medicine, vol. 47, no. 1, pp. 27–35.

[27] Bob Zhang, Jane, Y, & Fakhri, K 2012, "Detecting Optic Disc on Asians by Multiscale Gaussian Filtering", International Journal of Biomedical Imaging, vol. 2012, no. 1, pp. 1-10

[28] Angel Suero, Diego, M, Manuel, EGA & Jose MB 2013, "Locating the Optic Disc in Retinal Images Using Morphological Techniques", Proceedings of IWBBIO.

[29] Dehghani, A, Hamid, AM & Mohammad, SM 2012a, "Optic disc localization in retinal images using histogram matching", EURASIP Journal on Image and Video Processing, vol. 1, no. 1, pp. 1-11.

[30] Yu, H, Barriga, ES, Agurto, C, Echegaray, S, Pattichis, MS, Bauman, W & Soliz, P 2012, "Fast Localization and Segmentation of Optic Disk in Retinal Images Using Directional Matched Filtering and Level Sets", IEEE Transactions on Information Technology in Biomedicine, vol. 16, no. 4, pp. 644-657.

[31] Jaspreet Kaur & Sinha 2012, "Automated Localisation of Optic Disc and Macula from Fundus Images", International Journal of Advanced Research in Computer Science and Software Engineering, vol. 2, no. 4, pp. 242-249.

[32] Yang, Z, Tatham, AJ, Zangwill, LM, Weinreb, RN, Zhang, C & Medeiros, FA 2015, "Diagnostic ability of retinal nerve fiber layer imaging by swept-source optical coherence tomography in glaucoma", American journal of ophthalmology, vol. 159, no. 1, pp. 193-201.

[33] Goatman, GA, Fleming, AD, Philip, S, Williams, GJ, Olson, JA & Sharp, PF 2011, "Detection of new vessels on the optic disc using retinal photographs" IEEE Trans. Med. Imag., vol. 30, no. 4, pp. 972–979.

[34] Lu, S & Lim, JH 2011, "Automatic Optic Disc Detection From Retinal Images by a Line Operator" IEEE transactions on Biomedical Engineering, vol. 58, no. 1, pp. 88-94.

[35] Siddalingaswamy, PC, & Prabhu, GK 2010, "Automatic Localization and Boundary Detection of Optic Disc Using Implicit Active Contours" International Journal of Computer Applications, vol. 1, no. 7, pp. 1–5.

[36] Arturo, A, Manuel, EGA, & Diego, M 2010, "Detecting the Optic Disc Boundary in Digital Fundus Images Using Morphological, Edge Detection, and Feature Extraction Techniques", IEEE tran. on medical imaging, vol. 29, no. 11, pp. 1-9.

[37] Mahfouz, AE & Fahmy, AS 2010, " Fast localization of the optic disc using projection of image features", IEEE Transactions on Image Processing, vol. 19, no. 12, pp. 3285–3289.

[38] S Tobin, JKW 2006, “Characterization of the optic disc in retinal imagery using a probabilistic approach”, Proceedings of SPIE, vol. 61443.,

[39] Morris, T, Ritchings, T & Wood, I 2004, “Detection and Characterization of the Optic Disk in Glaucoma and Diabetic Retinopathy”, Medical Image Understanding and Analysis, vol. 2, no. 5, pp. 1-5.

[40] Xu, J, Chutatape, O, Sung, E, Zheng, C & Kuan, PCT 2007, “Optic disk feature extraction via modified deformable model technique for glaucoma analysis”, Pattern Recog., vol. 40, no. 1, pp. 2063–2076.

[41] Caroline, VSM, Elijah, BR, Kishore, KJ, Anandhic, D, Umberto, AS & Easter, SS 2015, “An empirical study on optic disc segmentation using an active contour model”, Biomedical Signal Processing and Control, vol. 18, no. 1, pp. 19-29.

[42] Karkuzhali, S, Manimegalai, D & Santhi, D 2015, “Effective Segmentation of Optic Disc in Retinal images for diagnosing Eye Diseases that leads to Blindness”, vol. 8, no. 1, pp. 427-434.

[43] Pradhepa, K, Karkuzhali, S, & Manimegalai, D 2015, “Segmentation and Localization of Optic Disc using Feature Match and Medial Axis Detection in Retinal Images”, vol. 8, no. 1, pp. 391–397.

[44] Ganesh babu, TR & Sathishkumar, R 2014, “Segmentation of Optic Nerve Head for Glaucoma Detection using Fundus images”, Biomedical & Pharmacology Journal, vol. 7, no. 2, pp. 697–705.

[45] Zhang, J, Yin, F, Wong, DWK, Liu, J, Baskaran, M & Cheng, CY, 2013, “Optic disk localization by a robust fusion method”, Proc. of SPIE Medical Imaging, vol. 8670, no. 8670, pp. 1-9.

[46] Kavitha, S & Duraiswamy,K 2013, “An Automatic Retinal Optic Disc Segmentation algorithm using differential windowing in the polar coordinate domain”, Australian Journal of Electrical and Electronics Engineering, vol. 10, no. 1, pp. 33-34.

[47] Joshi, GD, Sivaswamy, J, Karan, K & Krishnadas, SR 2010b, "Optic disk and cup boundary detection using regional information", Proc.of IEEE International Symposium on Biomedical Imaging: From Nano to Macro, pp. 948-951.

[48] N. Kleawsirikul, S. Gulati and B. Uyyanonvara, "Automated Retinal Hemorrhage Detection using Morphological Top Hat and Rule-based Classification", 3rd International Conference on Intelligent Computational Systems, April 2013.

[49] S. B. Junior and D. Walfer, "Automatic Detection of Microaneurysms and Hemorrhages in Color Eye Fundus Images", International Journal of Computer Science and Information Technology, Vol. 5, October 2013.

[50] R. V. Athira and D. F. Ferlin, "Detection of Retinal Hemorrhage using Splat Feature Classification Technique", International Journal Of Engineering Research and Applications, Vol. 4, pp. 327-330, January 2014.

[51] R. Inbarathi and R. Karthikeyan, "Detection of Retinal Hemorrhage in Fundus Images by classifying the Splat Features using SVM", International Journal of Innovative research in Science, Engineering and Technology, Vol. 3, pp. 1979-1986, March 2014.

[52] M. Reshma and M. Chavan, "Detection of Hemorrhages from Fundus Images using Hybrid Method", International Journal of Computer Applications, Vol. 12, December 2014

[53] A. Jadhav and P. Patil, "Classification of Diabetes Retina Images using Blood Vessel Area", International Journal of Cybernetics, Vol. 4, April 2015.

[54] A. W. Reza, C. Eswaran and S. Hari, "Automatic Tracing of Optic Disc and Exudates from color Fundus Images Using Fixed and Variables Thresholds", Journal of Medical Systems, Vol. 33, pp. 73-80, April 2008.

[55] A. Tripathi, K. K. Singh, B. K. Singh and A. Mehrotra, "Automatic Detection of Exudates in Retinal Fundus Images using Differential Morphological Profile", International Journal of Engineering and Technology, Vol. 3, pp. 2024-2029, July 2013.

[56] R. F. Mansour, E. Md. Abdelrahim and A. S. Al-Johani, "Identification of Diabetic Retinal Exudatesin Digital Color Images Using Support Vector Machine", Journal of Intelligent Learning Systems and Applications, pp. 134-142, August 2013.

[57] M. Akter, A. Rahman and A.K.M. Islam, “An improved method of automatic exudates detection in retinal images”, International Journal Innovative Research in Electrical, Electronics, Instrumentation and Control Engineering, Vol. 2, May 2014.

[58] N. Prakash, G. Hemalakshmi and M. Mary, “Automated Grading of Diabetic Retinopathy Stages in Fundus Images using SVM Classifier”, Journal of Chemical and Pharmaceutical Research, Vol. 8, 2016.

[59] J. Kuar and D. Mittal, “Segmentation and Measurement of Exudates in Fundus Images of the Retina for Detection of Retinal Disease”, Journal of Biomedical and Medical Imaging, Vol. 2, February 2015.

[60] D. Selvathi, and P. Lalitha Vaishnavi, “Gabor wavelet based blood vessel segmentation in retinal images using kernel classifiers”, International Conference onSignal Processing, Communication, Computing and Networking Technologies, pp. 830-835, 2011.